BOILING IN SELF-INDUCED RADIAL ACCELERATION FIELDS

By

ALI OWHADI

Bachelor of Science
University of Michigan
Ann Arbor, Michigan
1955

Master of Science
University of Michigan
Ann Arbor, Michigan
1956

Submitted to the faculty of the Graduate
College of Oklahoma State University
in partial fulfillment of the
requirements for the degree of
DOCTOR OF PHILOSOPHY
July, 1966

BOILING IN SELF-INDUCED RADIAL ACCELERATION FIELDS

Thesis Approved:

Kenneth J. Bell
Thesis Adviser

K C Chao

D. R. Haworth

Robert L. Robinson, Jr.

J. H. Boggs
Dean of the Graduate School

PREFACE

Boiling heat transfer to water at atomspheric pressure was studied in two helical coils with diameters of 9.86 in. and 20.5 in. The coils were constructed from 10 ft. lengths of 5/8 in. O. D. x 0.492 in. I. D. Inconel 600 tubing. The heat was supplied electrically. The ranges of liquid flow rate and heat flux studied were 77-306 lbs/hr and 19,000-81,000 Btu/(hr)(sq ft), respectively. Exit qualities up to 50 ^{o}F superheated vapor were covered.

Indebtedness is expressed to Dr. Kenneth J. Bell for his valuable guidance and inspiration supplied during this study. Acknowledgement is made of the helpful suggestions offered by the members of the Advisory Committee.

The author extends his gratitude to the Oklahoma State University and the State of Oklahoma for making their educational facilities available to students from abroad. Financial assistance was received from the Oklahoma State University.

Special thanks is due my wife, Soraya, whose patience and encouragement made this undertaking feasible.

TABLE OF CONTENTS

LIST OF TABLES

LIST OF FIGURES

CHAPTER I

INTRODUCTION

Because of its practical importance, boiling inside conduits under forced or natural circulation has been studied by many investigators. However, nearly all these studies have dealt with boiling in straight tubes. In view of the meager information available on boiling in coils and in view of the multitude of conditions and variables which could be investigated, the aim of the present work was to study experimentally the entire range of the vapor quality. Also, the ranges of the liquid feed rate and heat flux were to be extended to the limits of the capacity of the system.

It was felt that a rather broad approach would reveal some interesting characteristics of this geometry and indicate areas of future research which might be missed if the scope of the work were narrower. The system outlet pressure was, however, atmospheric in all the experiments, and only two coil diameters were investigated.

Boiling in a coil offers advantages in applications where the boiler product is to be 100 per cent vapor, namely:

(1) Once-through boilers to generate high quality steam for the secondary recovery of petroleum oils: In this application it is desirable to

vaporize as much of the feed water as feasible. The problem of water conditioning to avoid excessive solids deposition on the tube wall has been resolved in practice.

(2) Vaporizing rocket fuels such as liquid hydrogen: Here the fuel cools the engine as it evaporates. In a straight passage the transition from a wetted wall to a dry wall condition, and a subsequent sharp rise in the wall temperature, occurs at approximately 70 to 80 per cent vapor quality. In a coil this transition is delayed considerably; therefore, the low wall temperature can be maintained over a larger portion of the passage.

(3) Boiling in the absence of a gravitational field: In this case the strong self-induced radial acceleration assures the contact of the liquid with the heating surface.

The various modes of flow and heat transfer which occur in a straight vertical tube are reviewed in the following discussion and shown in Fig. I-1. With a subcooled liquid entering the tube, bubble nucleation may be absent in the entrance section. Low heat flux, high liquid velocity, and high subcooling favor the single-phase mode of heat transfer. As the liquid proceeds through the tube a radial as well as longitudinal temperature profile develops such that the liquid near the wall attains a temperature greater than that of the bulk liquid.

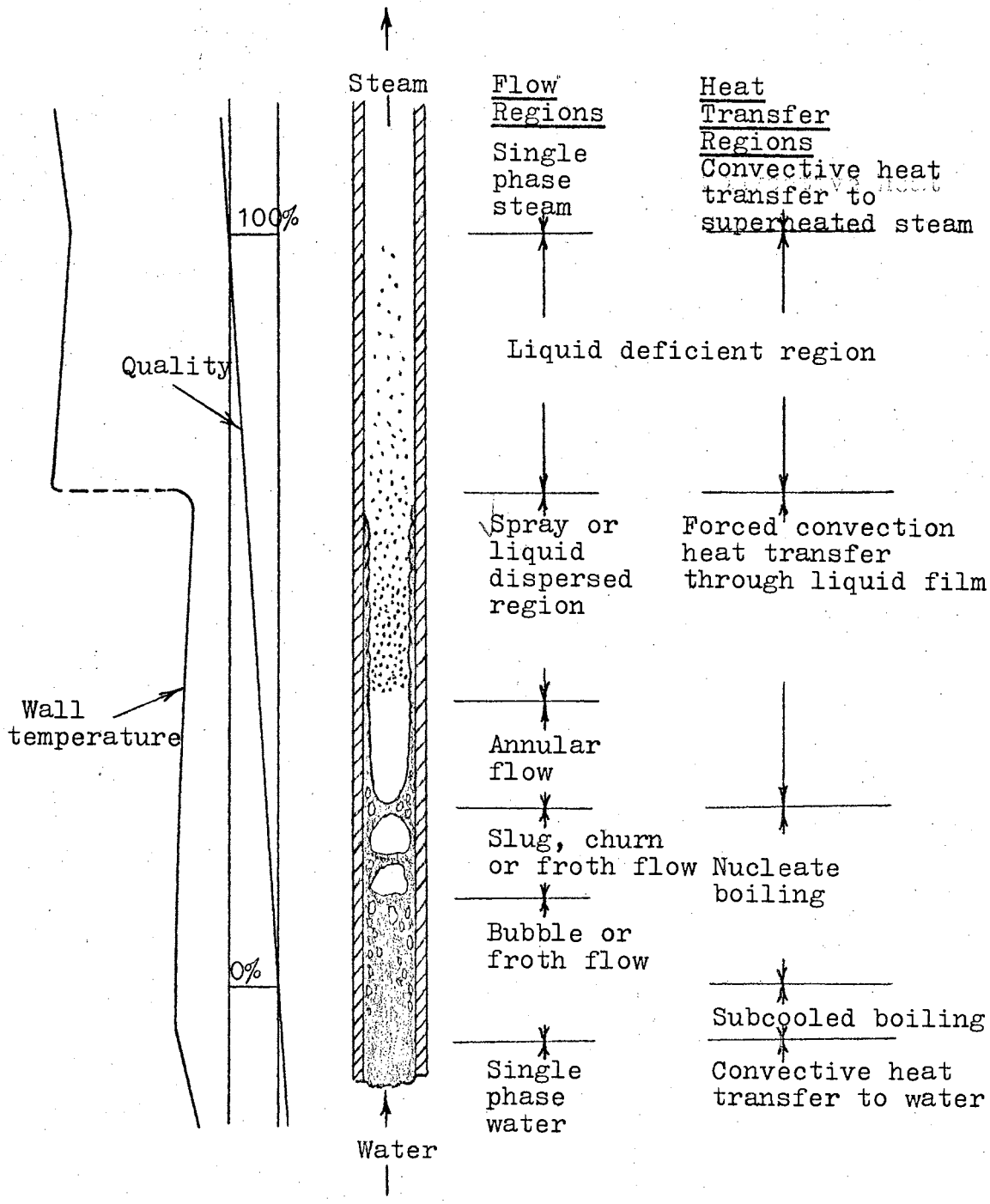

Fig. I-1. Various Regimes of Flow and Heat Transfer in a Straight Vertical Tube (Adapted from (5))

At some point bubble nucleation begins. As the bubbles grow and extend themselves into the colder region away from the wall, they transfer their latent heat to the cold liquid and collapse with no net generation of vapor—a mode variously known as "subcooled nucleate boiling," "local nucleate boiling," or "surface nucleate boiling." If a sufficiently high heat flux is imposed, it is possible to have subcooled film boiling.

When the bulk of the liquid reaches its saturation temperature, saturated nucleate boiling begins and net vapor is produced. At low vapor rates there will be individual bubbles flowing with the continuous liquid phase. This is the bubbly flow regime. As the vapor flow rate increases, the bubbles agglomerate and give rise to the plug flow regime where the diameter of the individual slugs of vapor becomes comparable to the tube diameter.

At higher vapor rates the core of the tube will be occupied mainly by the vapor and the liquid flows upward on the wall, but some liquid is entrained in the vapor core as droplets. In this regime—the annular flow regime—the heat transfer through bubble nucleation and growth gradually diminishes until the mechanism becomes principally convection with the resistance to heat transfer being in the liquid film.

At still higher vapor rates, all the liquid becomes entrained in the vapor phase in the form of fine droplets. This is called the mist flow regime. The liquid is brought

in contact with the wall by means of turbulent eddies. Any given spot on the surface is intermittently wetted by the liquid whereupon the liquid vaporizes and leaves the surface dry. Hence this region is also called the liquid-deficient region. The wall temperature fluctuates and rises until it reaches the Leidenfrost temperature, at which point the liquid can no longer wet the surface.

Beyond this point the heat transfer mechanism is that of convection to a gas, although liquid droplets are still present in the gas stream. As a result, the vapor is superheated and the transfer of heat from the vapor to the liquid droplets causes their gradual evaporation.

In the liquid-deficient region the rate of heat transfer is limited by the hydrodynamics of the system; therefore if the heat flux is constant throughout the tube, as would be the case with uniform electrical heating, and if the heat generated is in excess of the heat transferred, then the wall temperature must rise until a heat balance is established. Since the gas heat transfer coefficient is small, this temperature rise may be quite substantial, if not actually causing physical burnout.

Conditions in a coil differ from that of a straight tube in several respects, the most important of which is the presence of a self-induced radial acceleration. Let us first consider the flow of a single-phase fluid in a helical coil—a coil of constant radius of curvature. The fluid on the wall of the tube is at rest. The fluid near

the axis of the tube has a maximum velocity; therefore it is most strongly acted on by the centrifugal force which tends to throw the fluid outward. This fluid is replaced by the fluid around the wall moving inward. The net result is a secondary flow—a pair of symmetrical recirculation patterns—superimposed on the main flow (see Fig. I-2). This effect will be invoked later to present a picture of the liquid flow pattern when boiling takes place in a coil.

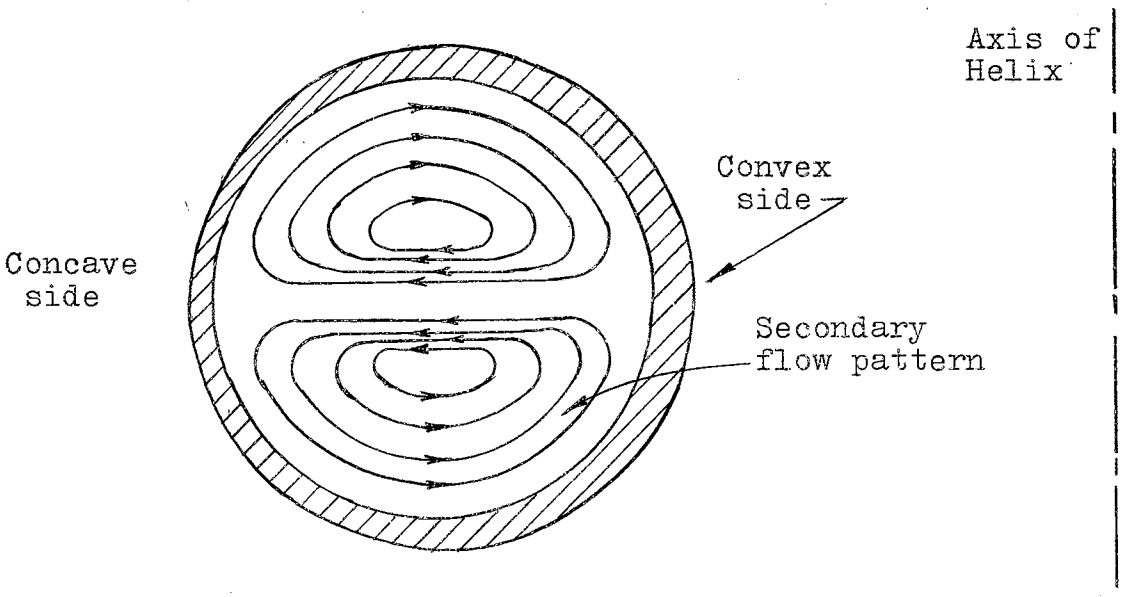

Fig. I-2. Secondary Flow in a Coil

Due to the presence of the centrifugal force, the pattern and the extent of the two-phase flow and heat transfer regimes outlined above are modified in a coil. In particular, the mist flow regime is suppressed and the transition from slug flow to annular flow occurs earlier than in a straight tube.

At first it seems plausible that the liquid should run on the concave side of the tube and the vapor on the convex

side. If this were the flow pattern, the convex side heat transfer coefficient should be of the order of that of vapor flowing in the coil tube. However, the measured temperatures and the heat transfer coefficients obtained from them indicate that this is not the case.

CHAPTER II

SURVEY OF LITERATURE

There is very little previous information on boiling in a coil, although there are a number of publications on heat transfer to and friction of a single-phase fluid in such geometry.

Two-Phase Heat Transfer

Hendricks and Simon (16) investigated heat transfer to sub-critical (two-phase), supercritical, and gaseous hydrogen in electrically-heated curved tubes at pressures of 100 to 600 psia, heat fluxes of 5.2×10^5 to 1.8×10^6 Btu/(hr)(sq ft), and radii of curvature of 2 to 7.5 inches. The qualitative results which they obtained were as follows: The heat transfer coefficient on the concave side can be as much as three times that on the convex side for the flow of near-critical hydrogen; two times that for gaseous hydrogen. Their near-critical and two-phase data indicated that the coefficient on the convex side was somewhat lower than that of a straight tube under similar conditions.

Carver et al. (3) conducted boiling experiments with water at 2600 psia in electrically-heated helical coils of 16 and 65 inches in radius and tube inside diameter of

0.42 inch. Their main purpose was to obtain data on the departure from nucleate boiling (DNB) in coiled tubes, particularly by comparison with that for a straight tube. Their results indicated that (1) the DNB steam quality was different for different positions around the circumference while being the same in a straight vertical tube; (2) a coiled tube has a higher average DNB steam quality than a straight tube; (3) departure from nucleate boiling is more gradual and the fluctuations in temperature are much lower in a coil than in a straight tube; (4) DNB steam quality for the small coil is higher than the large coil; (5) increasing the mass velocity increases the DNB steam quality.

Yudovich (36) experimented with boiling water and n-hexane in a helical coil made of $\frac{1}{2}$-inch copper tubing with a coil radius of 3 $\frac{1}{2}$ inches. Heating was effected by immersing the coil in a steam bath. He observed that for n-hexane runs and for water runs in the flow range of 5.1 to 17.5 lbs/hr the temperature of the superheated vapor leaving the coil increased with flow rate. At higher water flow rates, and partial vaporization of the feed, the average heat flux for the entire coil increased from 4,660 Btu/(hr)(sq ft) at 34.5 lbs/hr to 6,400 Btu/(hr)(sq ft) at 63.0 lbs/hr and then decreased to 4,360 Btu/(hr)(sq ft) at 113.5 lbs/hr.

No attempt was made by the above authors to correlate the local heat transfer coefficient as a function of their system parameters.

Single-Phase Heat Transfer

The study of heat transfer to single-phase fluids in coils dates back to 1925 when Jeschke (19) cooled air flowing up to Re = 150,000 in two coils having ratios of coil to tube diameter of 6.1 and 18.2. He correlated his data by

$$Nu = (0.039 + \frac{0.138}{D/d}) \, Re^{0.76}$$

Kirpikov (21) obtained data on four coils with D/d ratios of 10 to 18 and correlated his data in the range of $Re = 10^4$ to $Re = 4.5 \times 10^4$ by

$$Nu \, Pr^{-0.4} = 0.0456 \, Re^{0.8} \, (d/D)^{0.21}$$

The heat transfer coefficients were obtained using the temperature difference between the wall and the bulk. The properties were evaluated at the arithmetic average of the bulk temperature of the fluid at inlet and outlet. The heating agent was condensing steam.

Seban and McLaughlin (32) tested two electrically-heated coils with D/d ratios of 17 and 104 under laminar and turbulent conditions. They correlated their data in the turbulent range by

$$Nu \, Pr^{-0.4} = \frac{f}{2} \, Re$$

where f is the friction factor for a helical coil. The physical properties were evaluated at the film temperature. They noticed that the ratio of the heat transfer coefficient on the concave side to that of the convex side was of the order of two for turbulent flow while this ratio was higher in laminar flow.

Rogers and Mayhew (28) conducted heat transfer and pressure drop experiments with water in turbulent motion in helical coils heated by steam. Their results are only slightly different from Seban and McLaughlin's. Kubair and Kulor's (24) experiments were in the laminar range in helical and spiral coils. Wattendorf (33) obtained experimental data on wall shear stress and velocity distribution when an incompressible fluid was flowing in a curved channel of rectangular cross-section. Kreith (23) used Wattendorf's data and, from the analogy between momentum transfer and heat transfer, derived an expression for the Nusselt number for a curved surface; his derivation agrees with his experimental results of heat transfer from a curved surface.

Related Work

Rippel et al. (27) investigated isothermal pressure drop, hold-up and axial mixing in a helical coil of 8 inches in diameter made of ½-inch tubing. They studied the air-water system as well as others. Although their pressure drop data could be represented by the Lockhart-Martinelli (25) correlation, it was evident that the liquid rate was a parameter resulting in separate lines within the over-all correlation--an effect known previously (see discussion by Gazley and Bergelin at end of (25), based on data of (18)). The liquid hold-up fell below the Lockhart-Martinelli correlation. Axial mixing diminished with increasing

ratios of gas to liquid rate.

Koutsky and Adler (22) studied axial mixing in helical coils and noticed progressively stronger peaking of the residence time distribution curve with increasing Reynolds number, indicating increasingly stronger secondary flow effects.

Among other works related to the subject are successful attempts by Gambill et al. (12) to increase the burnout heat flux in a straight tube by inserting twisted metallic tapes in the tube to cause a swirling motion. Gambill and Green (13) achieved higher burnout heat fluxes by giving the liquid a vortex motion just before its entrance to the tube.

The effect of gravitational and radial acceleration on boiling has been studied by several investigators, e.g. Costello and Adams (6). Although there are conflicting results, most of them indicate that, other variables remaining constant, the heat flux increases approximately in proportion to the $\frac{1}{4}$ power of the acceleration.

CHAPTER III

EXPERIMENTAL SYSTEM

Forced convection boiling experiments were performed with water in two helical coils. The system exit pressure was atmospheric in both cases. A schematic diagram of the system is shown in Fig. III-1. The general arrangement of the apparatus is shown in Figs. III-2 and III-3.

The Coil

Two coils with radii of 4.93 and 10.28 inches, measured to the tube axis, were studied both of which were made of 10-foot lengths of 5/8-inch O. D. cold-drawn seamless tubing with a wall thickness of 0.068 inch. Inconel 600 was selected for the coil material because of its high electrical resistivity and its high melting range of 2500-2600 ^{o}F. The coil was mounted with its axis in the vertical direction. Heat was generated in the coil by passing a regulated DC current through it. The source of power was an AC-DC motor-generator, Lincolnweld SA-750, with a nominal capacity of 25 kilowatts output.

The electrodes were made of copper bars and were brazed to the coil. The coil was electrically insulated from the

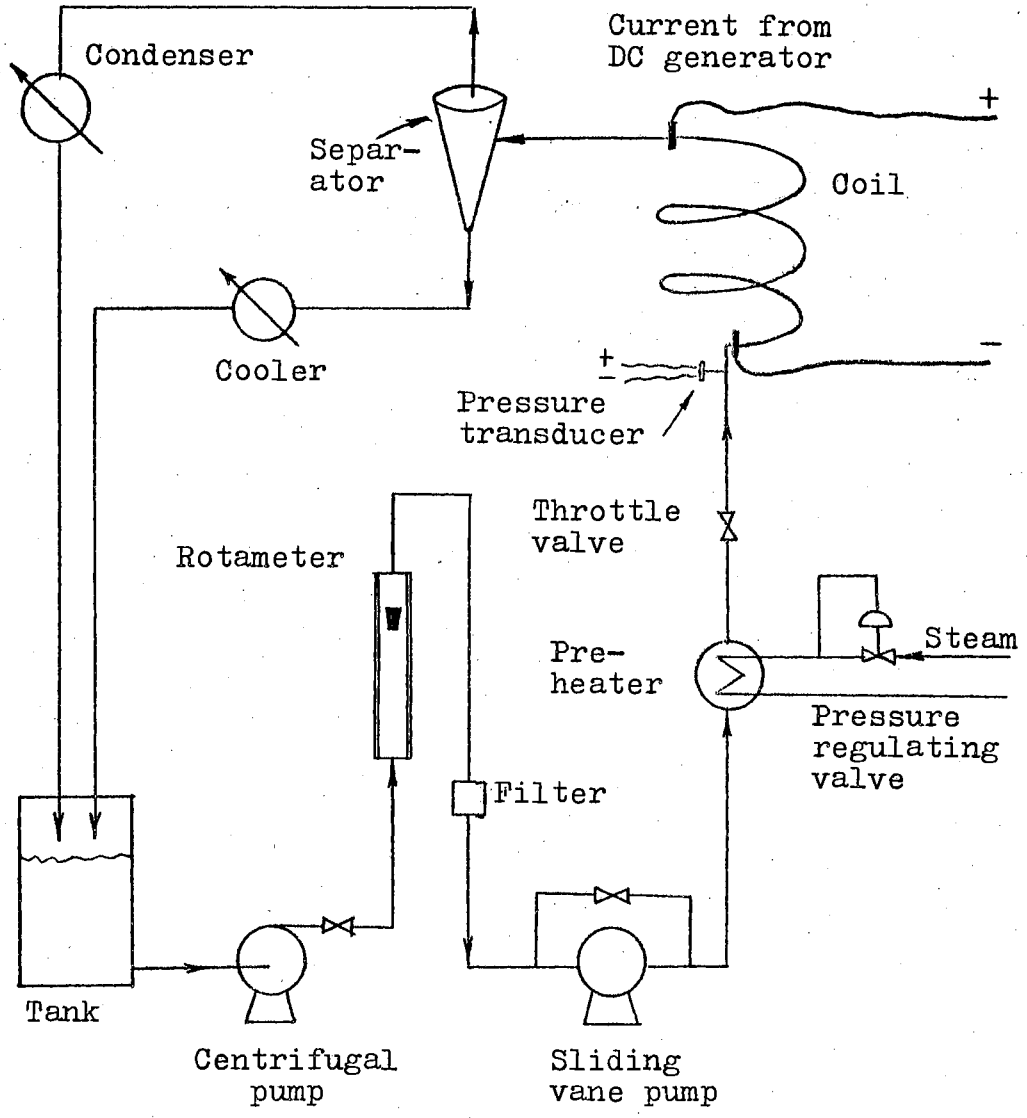

Fig. III-1. Schematic Diagram of the System

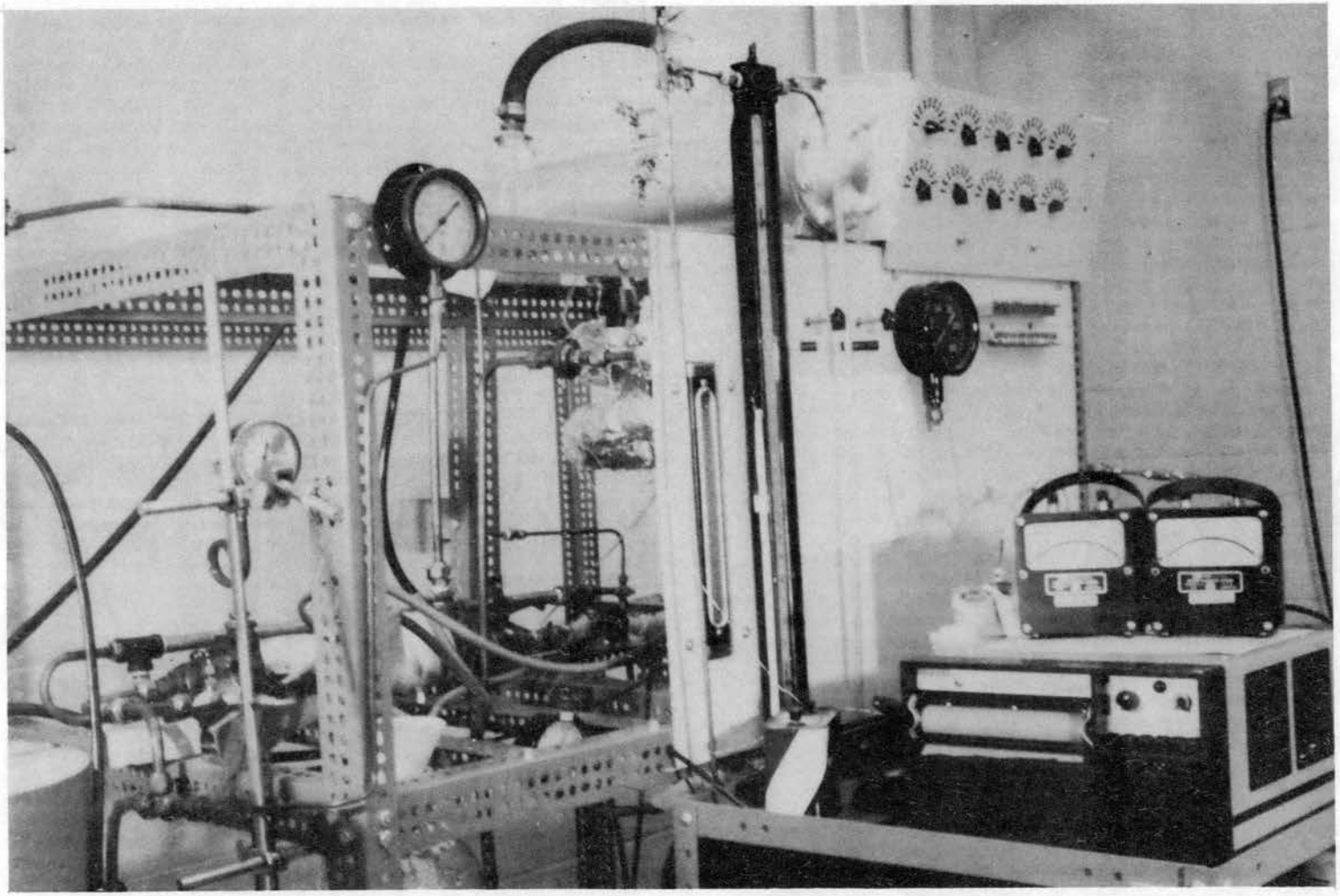

Fig. III-2. General Arrangement of the Apparatus, Front View.

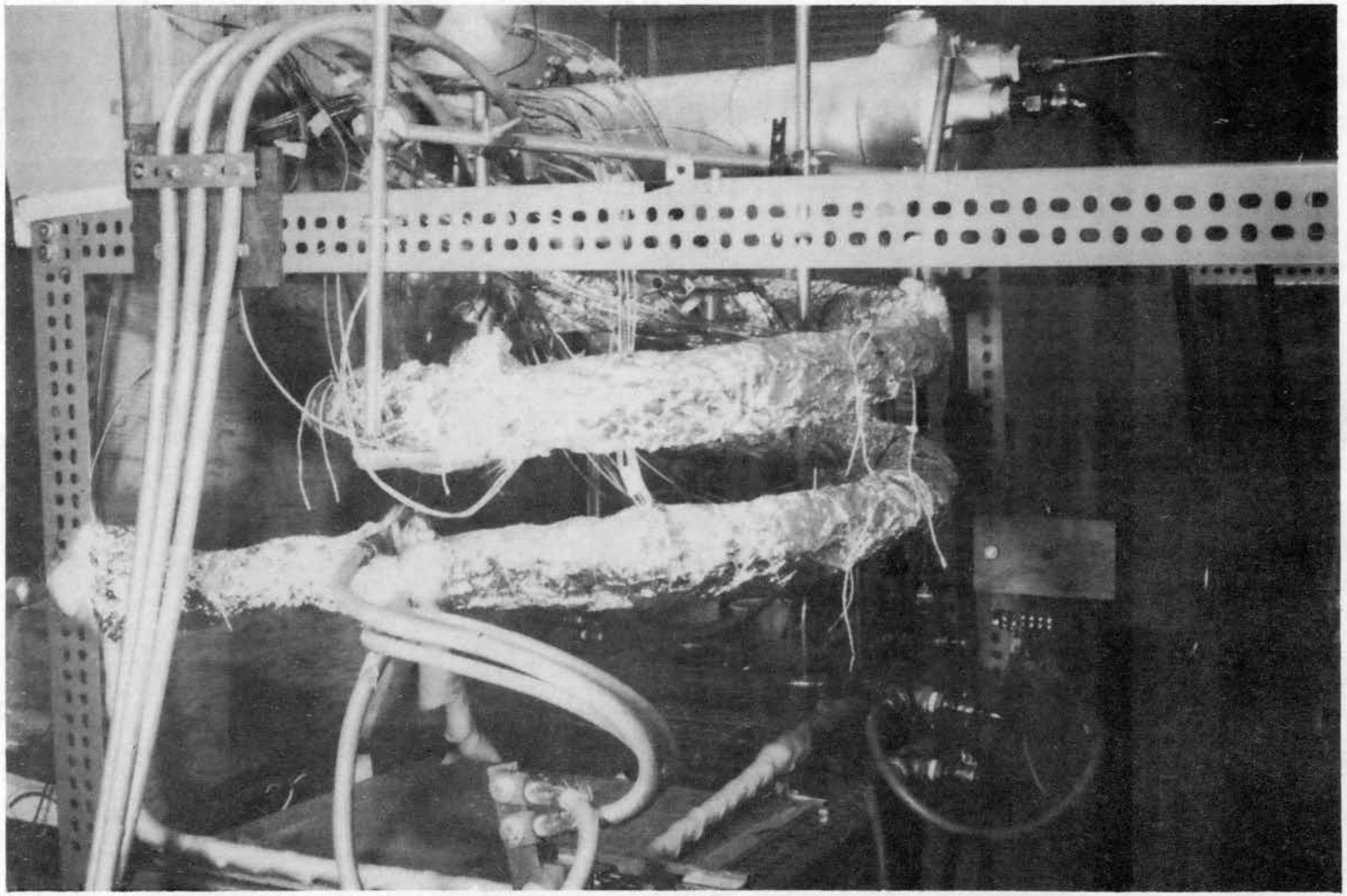

Fig. III-3. General Arrangement of the Apparatus, Side View.

rest of the system by inserting a short piece of silicone rubber tubing at each end of the coil. The resistance of the small coil was 0.0382 ohms and that of the large coil 0.0388 ohms. The electrical resistivity of Inconel 600 varies only 0.7 per cent over the range of 200 to 300 °F. This and other properties of Inconel 600 are tabulated in Appendix D.

The coils were cold-formed and then stress-relieved in a molten salt bath for three hours at 1400 °F. The tube was slightly flattened during bending as evidenced by the measurements of its major and minor diameters. However, no crimping was visible. The dimensions of the coils are listed in Table III-1.

TABLE III-1

COIL DIMENSIONS

	Small Coil	Large Coil
Coil diameter, inches center-to-center	9.86	20.57
Straight tube outside diameter, inch	0.629	0.629
Straight tube inside diameter, inch	0.492	0.492
Coiled tube major outside diameter, inch	0.637	0.631
Coiled tube minor outside diameter, inch	0.619	0.625
Distance between turns, inches center-to-center	3.9	4.6
Ratio of coil diameter to straight tube inside diameter	20.0	41.8
Heated length of coil, feet axial	9.35	9.35
Distance between thermocouple stations,* feet axial	1.00	1.00

* For both coils, the first thermocouple station was 1.10 ft (axial) from the inlet electrode.

After the thermocouples and the electrodes were connected to the small coil, a box was formed around the coil and filled with Vermiculite insulating material—a free-flowing granular form of expanded mica. The large coil was insulated with glass wool and then covered with aluminum foil.

Auxiliaries

Distilled water was drawn from a 5-liter glass container by means of a centrifugal pump and passed through a rotameter and a fine wire-mesh filter. A sliding-vane pump was used as booster pump capable of developing a head of 60 psi. Since the tolerances in the latter pump were very small, the filter was to guard against any metal chips reaching the pump. The maximum capacities of the rotameter, the vane pump, and the centrifugal pump were 200, 500, and 500 lbs/hr water, respectively. The effluent of the booster pump was sent to a shell-and-tube heat exchanger to preheat the feed to the desired temperature by condensing steam.

The preheated water was introduced to the coil where it was partially or totally vaporized. The vapor-liquid mixture was passed through a cyclone separator made of glass. The vapor was condensed in a shell-and-tube heat exchanger. The unvaporized portion of the feed, cooled by a double-pipe heat exchanger, and the condensate were returned to the feed tank through separate lines. All the lines and the pumps were made of copper, bronze, or brass.

Measuring Devices

The outside wall temperature of the coil was measured by iron-constantan thermocouples made of 20-gauge wire and cemented to the wall with Sauereisen cement. The thermocouples were electrically insulated from the coil by providing a thin layer of cement between the thermocouples and the coil. This was found necessary in order to avoid interference from the current in the coil.

The thermocouples were attached in such a way that they would rest on the coil for a distance of about 1 $\frac{1}{2}$ inches in order to minimize the conduction of heat away from the thermocouple junction. The thermocouples were held in place with clamps before applying the cement.

There were nine longitudinal thermocouple stations at intervals of one foot. At each station four thermocouples were installed around the circumference, each 90 degrees apart; therefore a total of 36 thermocouples measured the coil temperature. The numbering system of the thermocouples was as follows: Stations along the coil were numbered one through nine starting from the coil inlet. The four circumferential locations were numbered clockwise one through four, one being on the top of the tube (see Fig. III-4). Therefore, number 34, for example, refers to the thermocouple spaced three feet from the inlet and 270 degrees from the vertical position.

It should be noted that the coil axis was vertical

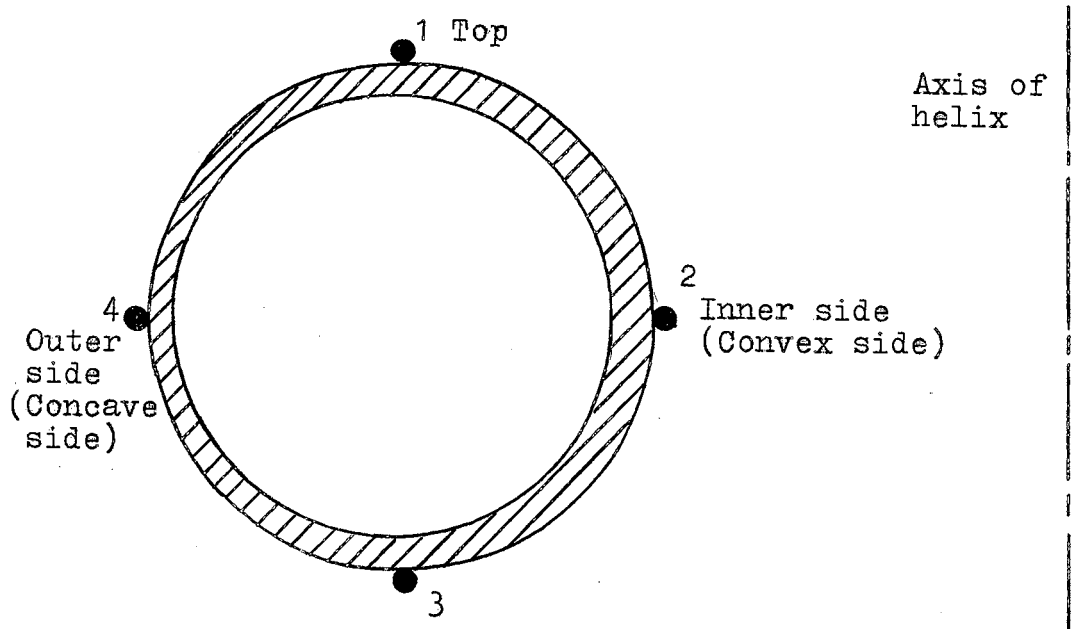

Fig. III-4. Circumferential Arrangement of Thermocouples at Each of Nine Longitudinal Stations

and the inlet at the bottom. The No. 2 location will be referred to as the convex side and the No. 4 as the concave side.

The thermocouples were brought to selector switches and then to the potentiometer. The selector switches were enclosed in a box to maintain a uniform temperature at the switches. A steam bath was used for the reference junction in all the temperature measurements. Since the saturation temperature was calculated from pressure measurements, the changes in the atmospheric pressure would cause an error in the saturation temperature. The purpose of the steam bath for the reference junction was to avoid this error, which could be as much as 2 ^{o}F. Considering that the primary interest was in the difference between the wall temperature and the saturation temperature, this procedure

was felt satisfactory, although a more conventional method would be to use ice for the reference junction and measure the atmospheric pressure in each run. Small errors resulting from the present method of temperature measurement are discussed in Appendix H.

The inlet pressure of the system was measured with a mercury manometer as well as a strain gauge pressure transducer—Consolidated Electrodynamics Corporation Model 4-316-001. Pressures along the coil were measured with the manometer only. The transducer was used to detect pressure oscillations. It had a range of 0-50 psig and an output of 0-20 millivolts. The transducer circuit is shown in Fig. III-5.

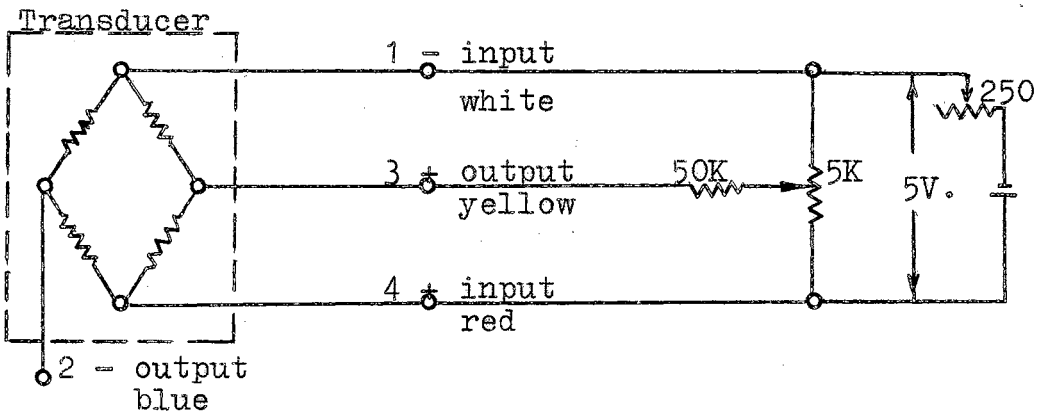

Fig. III-5. Pressure Transducer Circuit Diagram

The output of the pressure transducer was recorded on an 18-channel oscillograph, a Consolidated Electrodynamics Model 5-124. The sensing elements in these oscillographs are D'Arsonval-type galvanometers which deflect a light beam on a photo-sensitive paper. The extent of deflection is proportional to the input current rather than its voltage; therefore each galvanometer had to be calibrated for a given circuit resistance.

The output of the various thermocouples could also be recorded on the oscillograph. The specifications of the galvanometers used for recording the pressure and the temperature are listed in Appendix J.

The other temperatures that were measured were the water temperature at the coil inlet and the vapor temperature after the cyclone separator.

The current intensity was measured with a Weston Model 931 ammeter in conjunction with a shunt having a range of 0-750 amps DC. The current potential was measured with a Weston Model 931 voltmeter having a range of 0-50 volts DC. These meters were calibrated by the manufacturer.

CHAPTER IV

EXPERIMENTAL PROCEDURE

Calibration of Thermocouples

The thermocouples were first calibrated against a platinum resistance thermometer certified by the National Bureau of Standards. The iron-constantan thermocouples and the N.B.S. thermometer were placed in a silicone oil constant temperature bath and compared at 200, 260, 320, and 420 ^{o}F. The maximum deviation from the N.B.S. thermometer was always less than 1 ^{o}F and usually much less.

When the thermocouples were installed on the coil it was noticed that these calibrations did not hold. This was attributed to the conduction of heat through the thermocouple wires and to the limited area of contact between the thermocouples and the coil surface. Therefore, a new set of calibrations was obtained by bleeding steam through the coil and making measurements after one hour and after 24 hours. There was no noticeable difference between the readings after one hour and after 24 hours.

In order to make appropriate corrections for temperatures higher than 212 ^{o}F, it was assumed that the deviation from the true reading was due to conduction in the wires

which in turn was proportional to the difference between the thermocouple junction temperature and the ambient temperature. Thus it was assumed that the thermocouple correction was also proportional to this temperature difference. In this manner every thermocouple had its own correction depending on its temperature. The calibrations of the thermocouples at the atmospheric condensing temperature of steam are shown in Appendix I.

Since the great majority of the data were taken below 300 ^{o}F, and since the original calibration of the thermocouples against the N.B.S. thermometer showed small deviations, it is felt that the above procedure caused a maximum error of 0.2 ^{o}F in the measurement of the coil surface temperature.

The calibrations of the thermocouples were periodically checked; only thermocouple No. 94 of the small coil showed a changing calibration with time so that near the completion of the runs it had a calibration of -0.145 millivolts. When the coil was removed it was noticed that this thermocouple had separated from the surface of the coil. All the other thermocouples appeared intact. At this time it was also noticed that thermocouple No. 74 was cemented somewhat away from its intended position and closer to No. 73, which explains the fact that this thermocouple gave consistently low readings.

Oscillograph Calibration

Since the galvanometers in the oscillograph are current sensitive, their deflection was adjusted by varying the circuit resistance. Calibration was accomplished by introducing a known voltage, the output of a thermocouple in this case, which was read on the potentiometer. An arrangement was provided for the thermocouple output to be fed to the galvanometer through two parallel circuits—one for the high temperature range and one for the low. The low range circuit caused the light beam to be deflected 0.1 inch per 0.03 millivolt while the high range circuit gave the same deflection per 0.1 millivolt.

The output of the pressure transducer was fed to a separate galvanometer and the circuit resistance was adjusted such that 1.0 psi caused the light beam to be deflected 0.1 inch.

Rotameter Calibration

The rotameter had a range of 0-200 pounds water per hour. It was calibrated by measuring the volume of water collected in a graduated cylinder over a period of time and measuring its temperature. The rotameter calibration is shown in Appendix I.

It was discovered, however, that the rotameter calibration changed as much as 2 per cent due to the changes in the water temperature. It was decided to use the

rotameter as a guide only and to measure the flow rate by timing the effluent for every run. The flow rate measurement was usually repeated three times and averaged. Its repeatability was always within 1 per cent and usually within 0.5 per cent.

Execution of Runs

The runs were started by setting the pump by-pass valve to give the desired flow rate. Fine adjustments were made later in the run. The generator voltage had a tendency to drift back in the beginning of the run. For this reason it usually required 1 $\frac{1}{2}$ hours of time to warm up and maintain a steady voltage. The feed water temperature was adjusted by regulating the pressure of steam to the preheater. Care was taken to maintain the water pressure in the preheater above its saturation pressure.

The thermocouple outputs as well as the pressure transducer output were read on a Leeds and Northrop Model 8686 potentiometer. These voltages were recorded on the oscillograph in some runs.

The inlet pressure of the coil was read on a U-tube mercury manometer. After the temperature measurements were made on the small coil, the thermocouples were removed and 1/32-inch pressure taps were drilled in the coil at stations 1, 3, 5, 7, and 9 on the top of the tube, i.e., location No. 1. An additional hole was drilled at the location No. 4 of station No. 9. These pressures and the inlet pressure

were read on the mercury manometer at the same power input as when temperature measurements were made.

All the temperatures were read twice to assure steady state conditions. Some runs were repeated after several weeks to see if the results changed due to surface aging; no change was noticed.

The water was occasionally analyzed for its oxygen content. Since usually 1 $\frac{1}{2}$ hours of boiling preceded any temperature measurement and since the total system hold-up was only 6 liters, less than 2 ppm oxygen was found in the water.

The system was drained and refilled with distilled water several times prior to the first run and a few times thereafter in order to minimize the solids content of the water.

CHAPTER V

EXPERIMENTAL RESULTS

In this chapter the experimental results on heat transfer to single-phase water in the laminar and turbulent regimes, subcooled boiling, two-phase heat transfer, two-phase pressure drop, and the stability of the two-phase system are presented in the above order. In the next chapter, the two-phase heat transfer and pressure drop data are correlated and discussed.

Single-phase Heat Transfer

The stabilizing effect of the secondary flow is to delay the transition from laminar to turbulent flow. Ito (17) recommends the following formula for the onset of turbulence in a helical coil:

$$(Re)_{cr} = 2 \times 10^4 \left(\frac{d}{D}\right)^{0.32} \qquad (V-1)$$

According to this formula the critical Reynolds number for the small coil should be 7660 and for the large coil 6060.

One run with each coil was made with water in laminar flow, the results being plotted in Figs. V-1 and V-2. In both cases subcooled boiling occurred near the exit where the inside wall temperatures were 214-220 ^{o}F. This gave rise to higher heat transfer coefficients for these points.

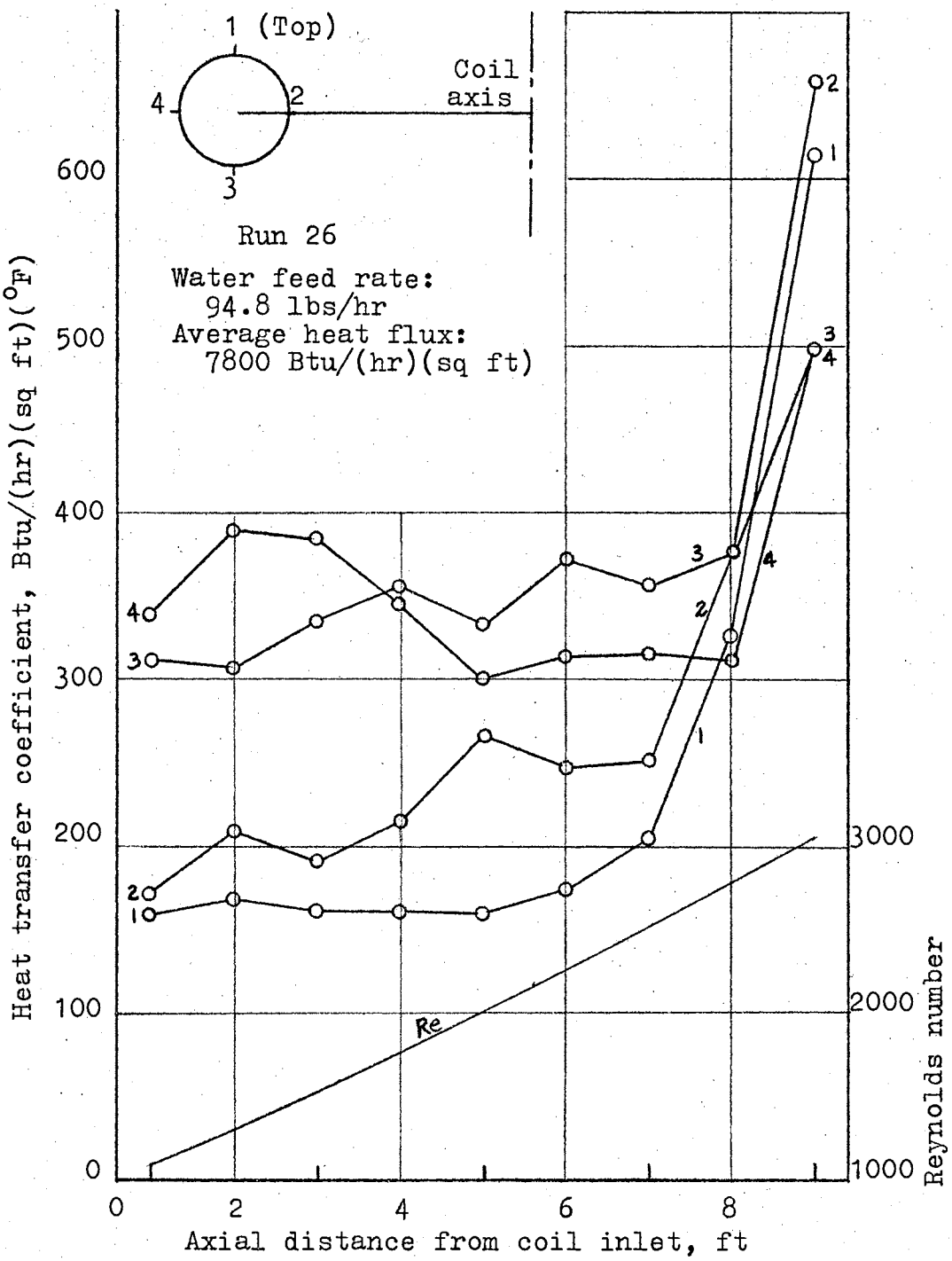

Fig. V-1 Heat Transfer to Water in Laminar Flow in Small Coil

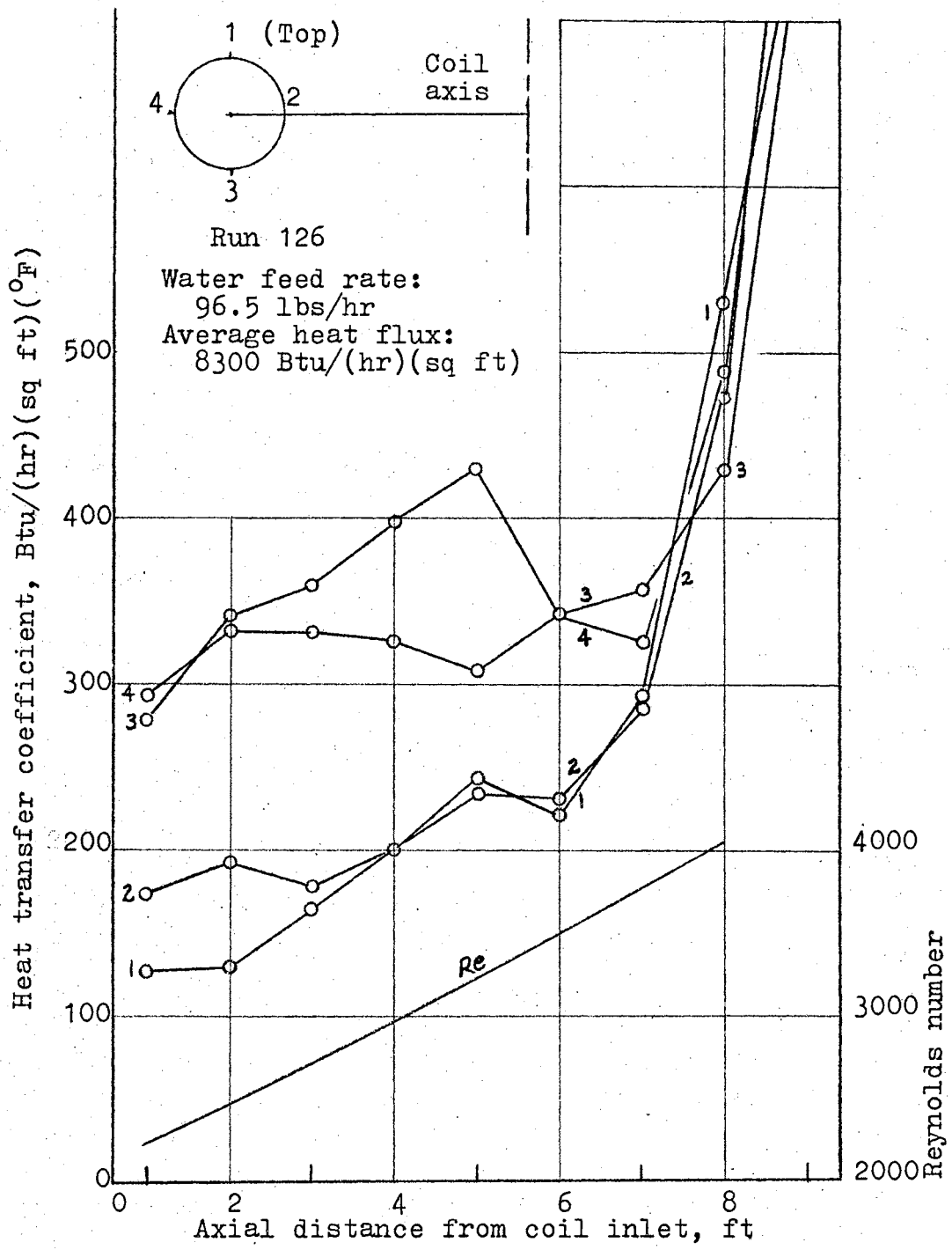

Fig. V-2 Heat Transfer to Water in Laminar Flow in Large Coil

In order to be well within the laminar regime, the water velocity was kept low--0.33 ft/sec in both runs. As a result, natural convection had a significant effect as evidenced by the low values of the heat transfer coefficient at the top of the tube (point 1) compared to the bottom of the tube (point 3). The difference between the heat transfer coefficients for the points 2 and 4 is not as large here as reported in (32).

The values of the circumferential average heat transfer coefficient calculated from these runs were about three times the asymptotic values predicted from Seban and McLaughlin's (32) equation:

$$\frac{hd}{k_l} (Pr)^{-1/3} = 0.13 \left[\frac{f}{8} (Re)^2 \right]^{1/3} \qquad (V-2)$$

which is based on experimental values obtained from laminar flow of liquids having a Prandtl number of 100-657. In the above equation f is the friction factor calculated from White's formula (34):

$$\frac{f}{f_s} = \left[1 - \left(1 - \left(\frac{11.6}{Re\ (d/D)^{\frac{1}{2}}} \right)^{0.45} \right)^{2.22} \right]^{-1} \qquad (V-3)$$

where

$$f_s = 64/Re.$$ ← This is not the Fanning friction factor

The large discrepancy is perhaps due to natural convection and the substantially lower Prandtl number of water, in which range no correlation is available.

Runs 22, 25, and 125 were performed with water flowing in the turbulent regime. The results of Runs 25 and 125

are shown in Figs. V-3 and V-4, respectively. The ratio of the heat transfer coefficient of point 4 to that of point 2 is approximately 2.8 for the small coil and 2.2 for the large coil. Again, subcooled boiling first occurs at points 1 and 2 in Run 125. In Run 25 the wall temperature was always below 212 ^{o}F; therefore, no subcooled boiling could take place. A significant entrance effect is noticed for point 4 of the small coil.

The circumferential average heat transfer coefficients calculated for the two coils agree well with the data of Seban and McLaughlin (32) and Rogers and Mayhew (28), both of which were correlated by

$$Nu = 0.023\ Re^{0.8}\ Pr^{0.4}[Re^{1/20}(\frac{d}{D})^{1/10}] \qquad (V-4)$$

where the liquid properties were evaluated at a film temperature defined as the average of the bulk temperature and the circumferential average temperature of the wall. The mean deviation of the circumferential average heat transfer coefficient in the turbulent runs from the values predicted by Eqn. (V-4) was approximately 5 per cent.

Subcooled Boiling

Runs 24 and 124 were conducted under higher heat flux than the single-phase runs. Thus, at some points along the coil the inside surface temperature was sufficiently above the saturation temperature for subcooled boiling to take place. As in the previous runs, subcooled boiling first occurs at points 1 and 2 and later at 3 and 4 (see Figs.

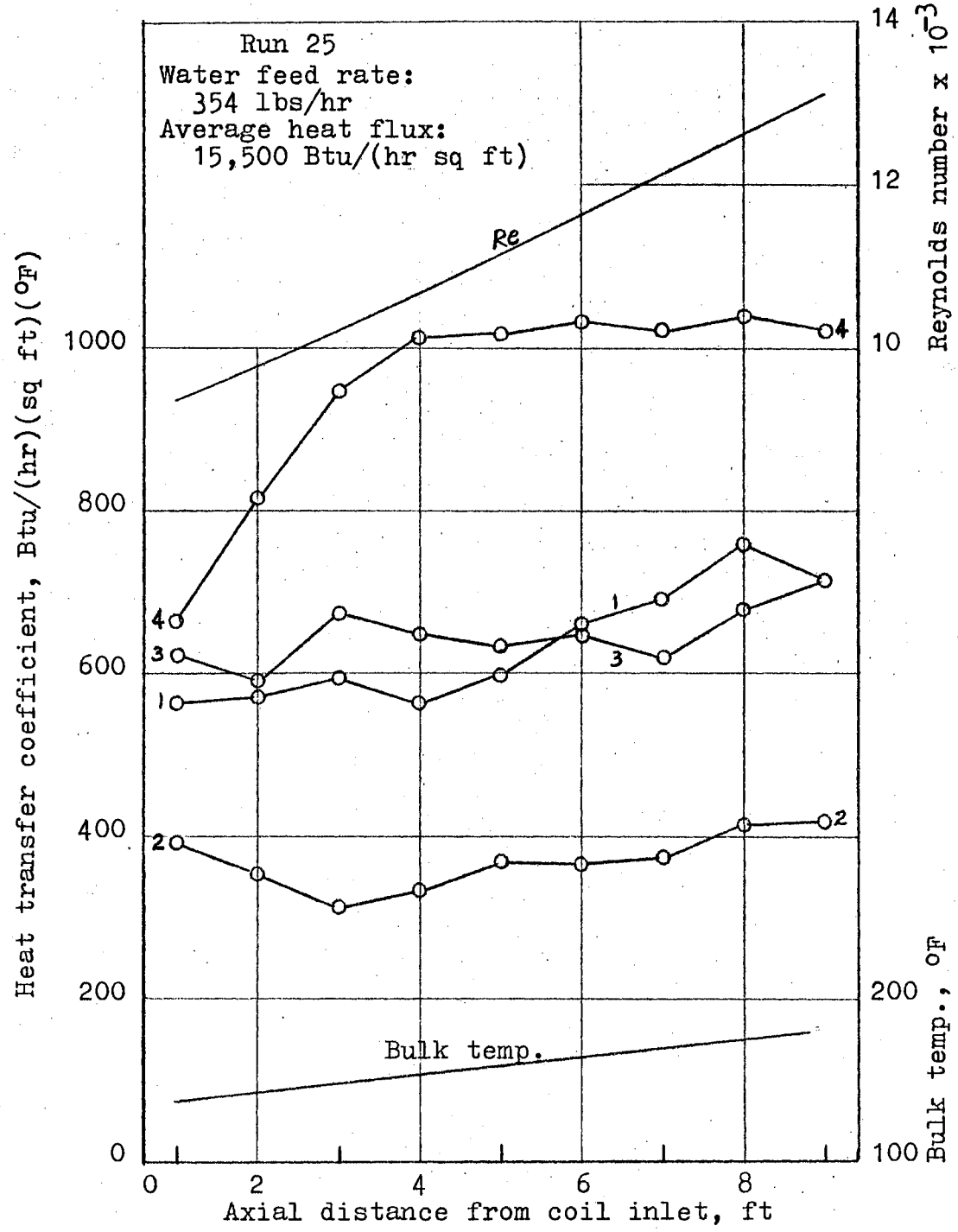

Fig. V-3 Heat Transfer to Water in Turbulent Flow in Small Coil

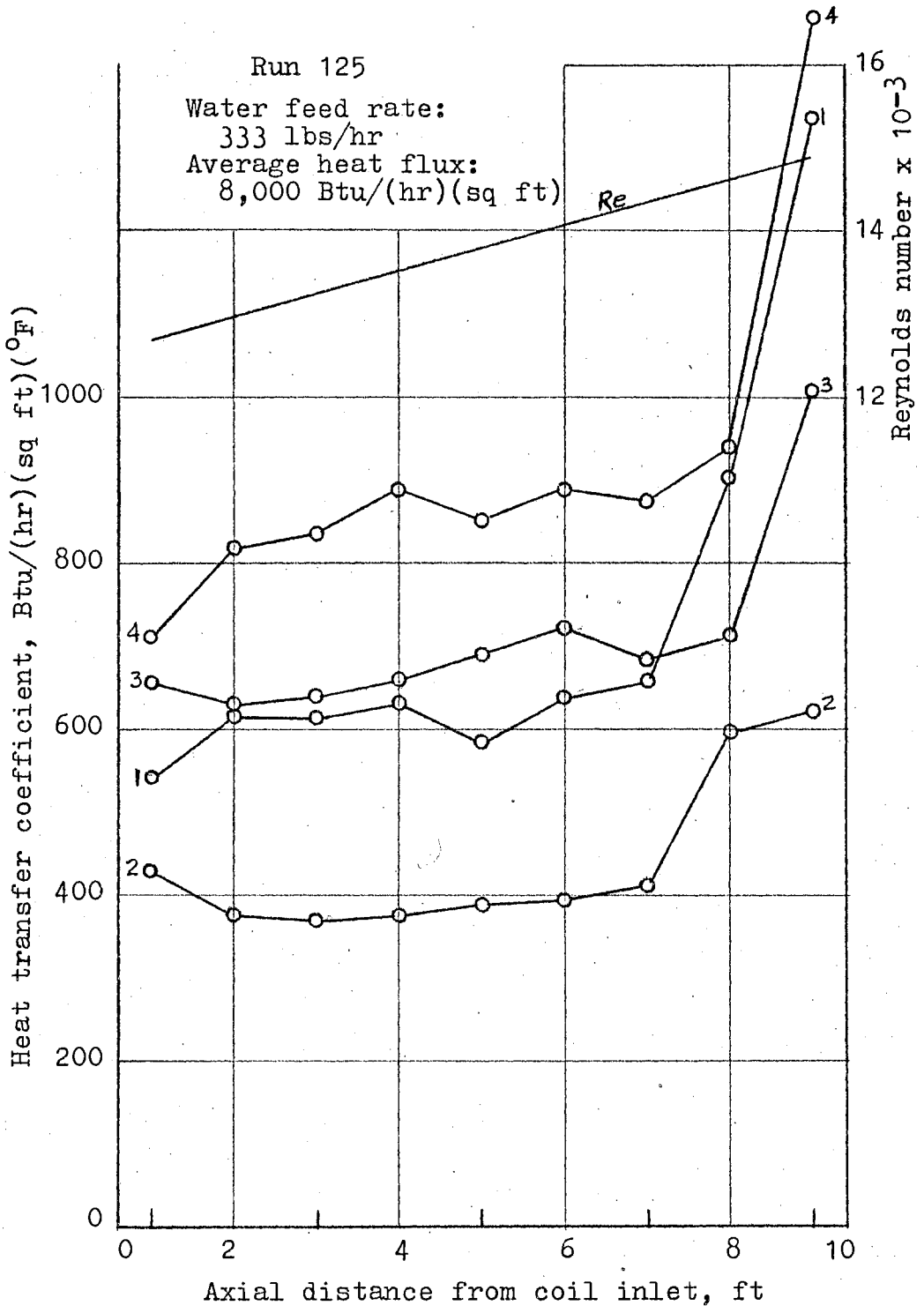

Fig. V-4 Heat Transfer to Water in Turbulent Flow in Large Coil

V-5 and V-6).

The heat transfer coefficient in these runs is based on the temperature difference between the wall and the mixed mean liquid temperature—bulk temperature. The fact that the calculated heat transfer coefficient for point 1 is less than that of point 3 at the entrance to the coil can be explained by the influence of natural convection which tends to maintain a higher local liquid temperature near the top of the tube. Further downstream the liquid temperature becomes sufficiently high to allow bubble growth on the surface; since the local liquid temperature is higher near the top of the tube, bubble growth is enhanced and the result is a higher heat transfer coefficient for point 1 compared to the others.

Two-phase Heat Transfer

The experiments in this category, which constitute the main part of this investigation, were intended to cover as large a range of vapor quality as feasible. The liquid feed rate and the heat input were arranged in such a way that the exit quality would be the same in certain runs as shown in Figs. V-7 and V-8. Runs 18, 19, and 20 were made at increasingly higher exit qualities until the exit vapor was 48 degrees superheated in Run 20. Similarly, the exit vapor in Run 120 was 50 degrees superheated. Runs 11, 12, 15, 10, 9, and 13 were unstable, i.e., the system pressure and temperature oscillated with a definite period.

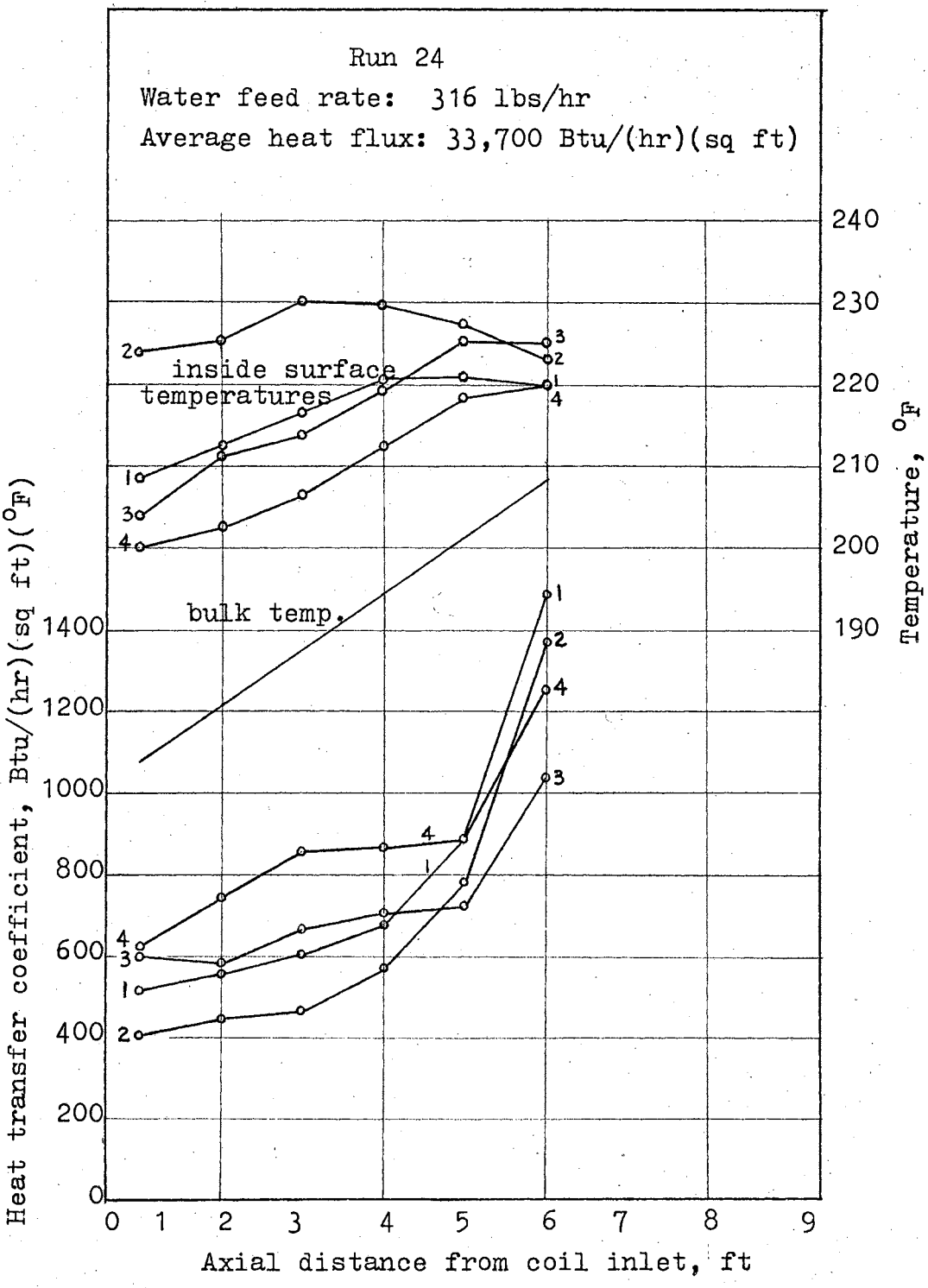

Fig. V-5 Subcooled Boiling in Small Coil

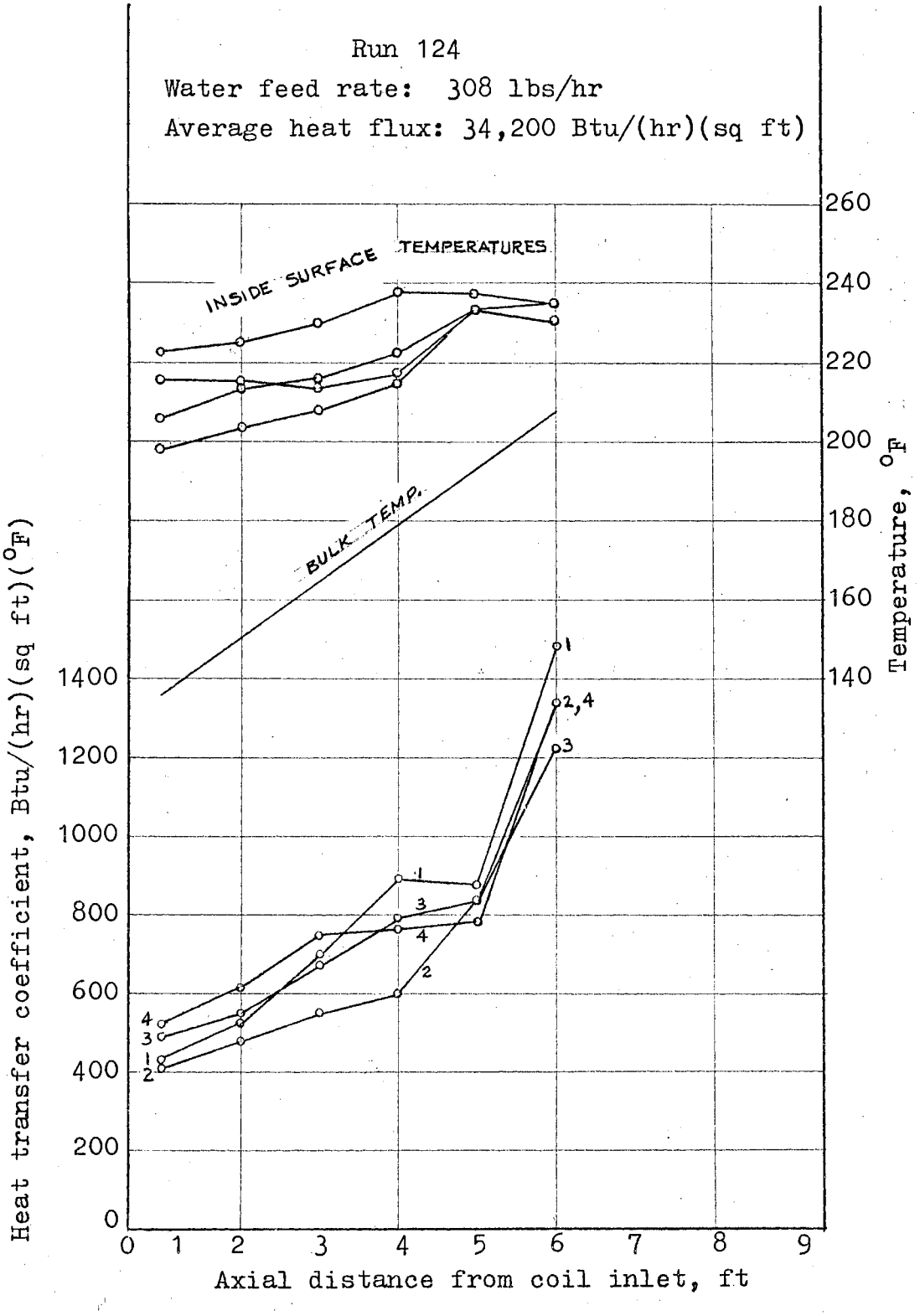

Fig. V-6 Subcooled Boiling in Large Coil

Flux / Flow	8000	12,600	20,400	32,200	51,000	81,000
31	(11) 32%	(12) 50%	(15) 80%		unstable	
49		(10) 32%	(9) 50%	(13) 80%		
78			(3) 32%	(4) 50%	(14) 80%	(18) (19) (20)
124			(27)	(7) 32%	(8) 50%	(16) 80%
197			(28)	(29)	(6) 32%	(5) 50%
306			(21)			

Notation:

Flux: average heat input based on inside surface area, Btu/(hr)(sq ft)

Flow: liquid feed rate, lbs/hr

Circled numbers refer to run numbers.

Numbers below circles denote exit steam quality.

Fig. V-7 Plan of Runs For Small Coil, Saturated Boiling Runs

Flow \ Flux	8,000	12,600	20,400	32,200	51,000	81,000
31						
49						
78				(104) 50%	(114) 80%	(119) (120)
124			(127)	(107) 32%	(108) 50%	(116) 80%
197			(128)	(129)	(106) 32%	(105) 50%

Notation:

Flux: average heat input based on inside surface area, Btu/(hr)(sq ft)

Flow: liquid feed rate, lbs/hr

Circled numbers refer to run numbers.

Numbers below circles denote exit steam quality.

Fig. V-8 Plan of Runs For Large Coil, Saturated Boiling Runs.

The results of Runs 4, 104, 16, 116, 19, 119, 20, 120, and 21 are presented in this chapter in graphical form as representative runs (Figs. V-9 through V-17). The data for all the runs are reported in Appendices E and F. The circumferential average heat transfer coefficients for all the stable runs for the small coil are shown in Fig. V-18 and for the large coil in Fig. V-19.

Near the coil inlet, in general, the heat transfer coefficient was highest for point 2 and lowest for point 4. This is due to the varying extent of nucleate boiling around the circumference. Because of the deformation of the tube in bending, the wall thickness and heat generation are highest at point 2 (see Appendix A). Therefore, point 2 has the highest radial heat flux and inside wall temperature. The higher wall temperature gives rise to a larger nucleate boiling component at point 2 compared to the other three points. Since the nucleate boiling heat flux is proportional to ΔT^a, where a is usually larger than two, the heat transfer coefficient for point 2 is higher than the other points, even though its ΔT is the highest of the four.

At approximately 2 feet from the inlet, often the heat transfer coefficient went through a minimum. This was particularly true of point 2. This behavior was thought to be a result of the suppressing effect of turbulence on nucleation, causing a drop in the nucleate boiling component while not enhancing the convective component to a comparable extent. The total heat transfer is assumed to consist of a

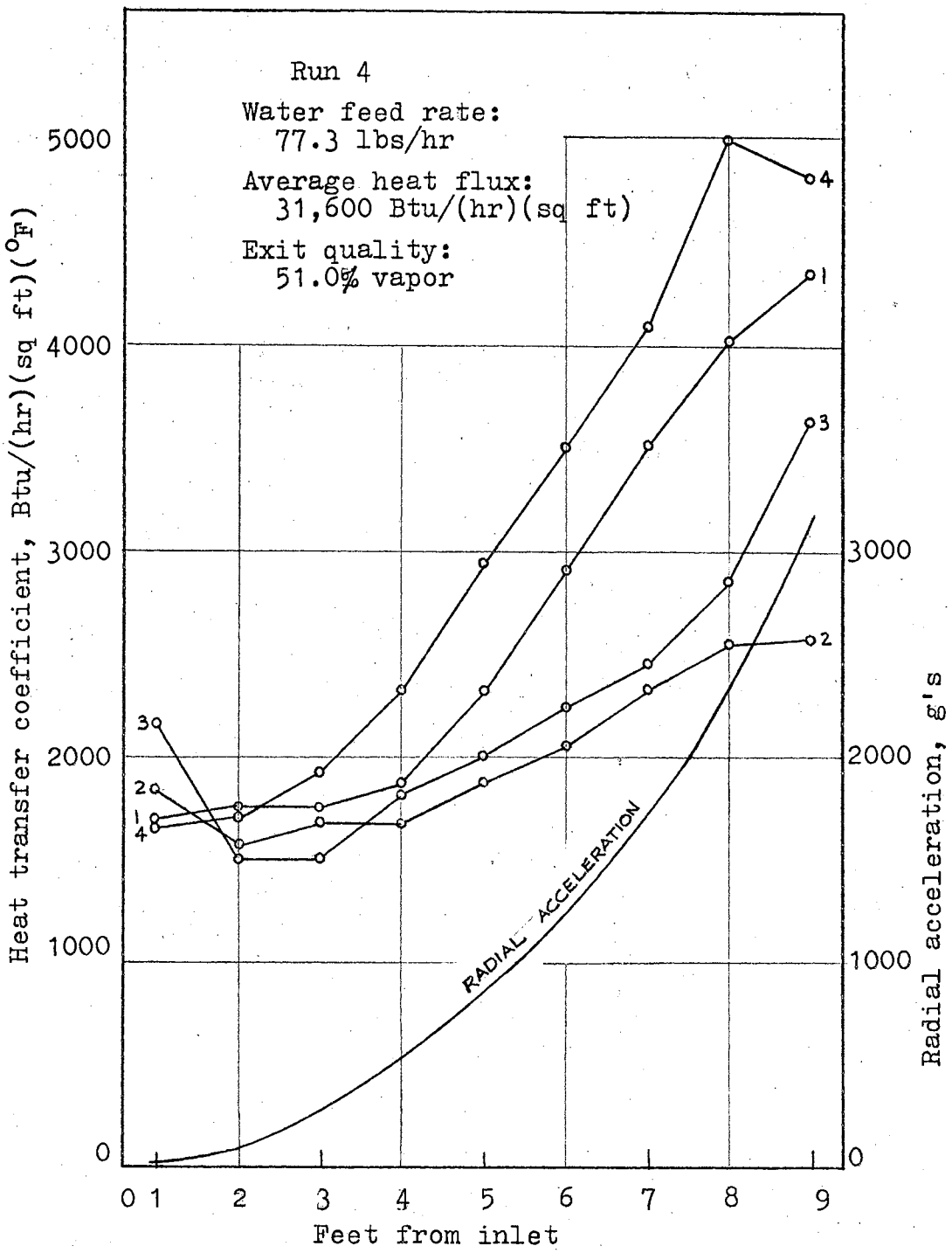

Fig. V-9 Saturated Boiling in Small Coil, Low Feed Rate

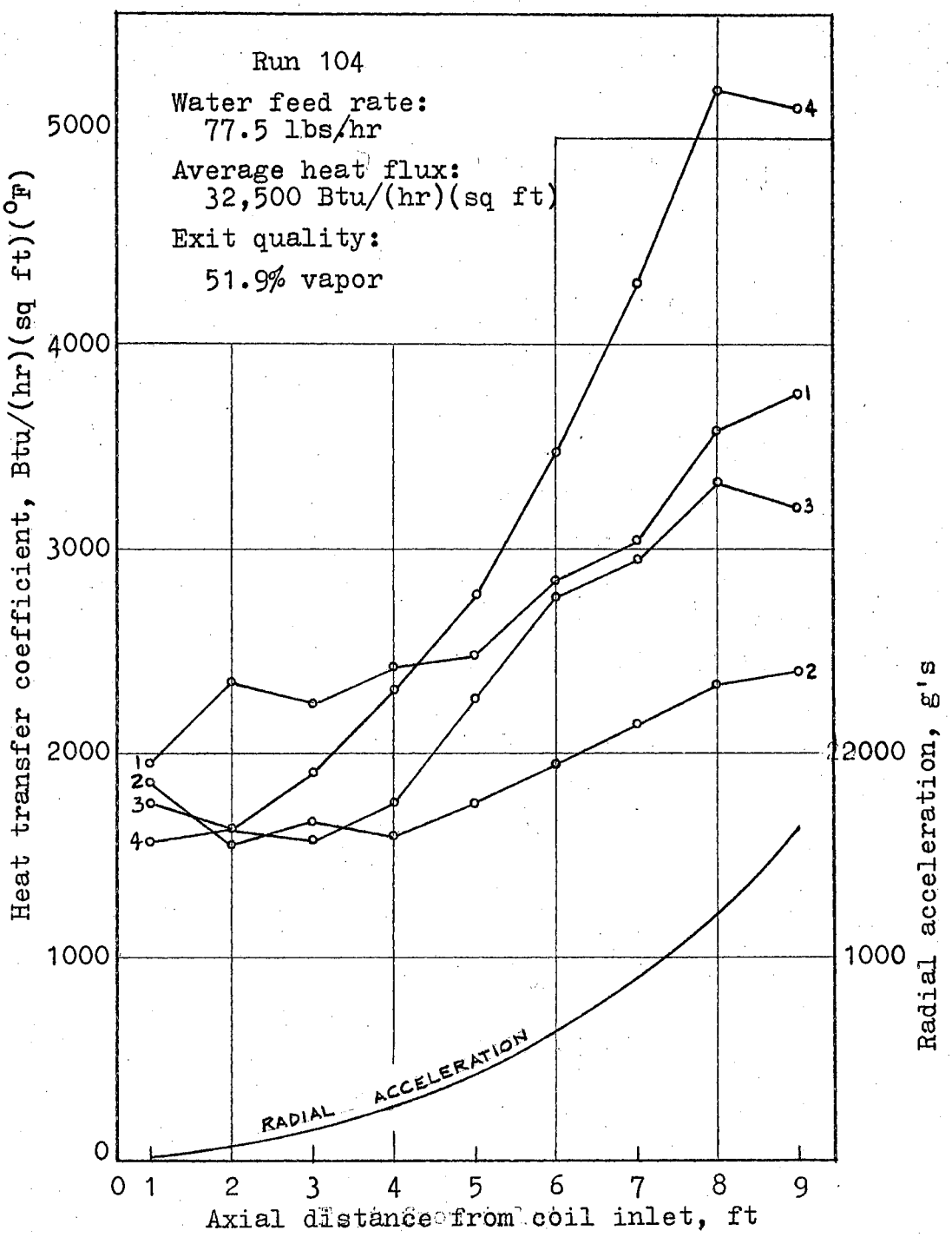

Fig. V-10 Saturated Boiling in Large Coil, Low Feed Rate

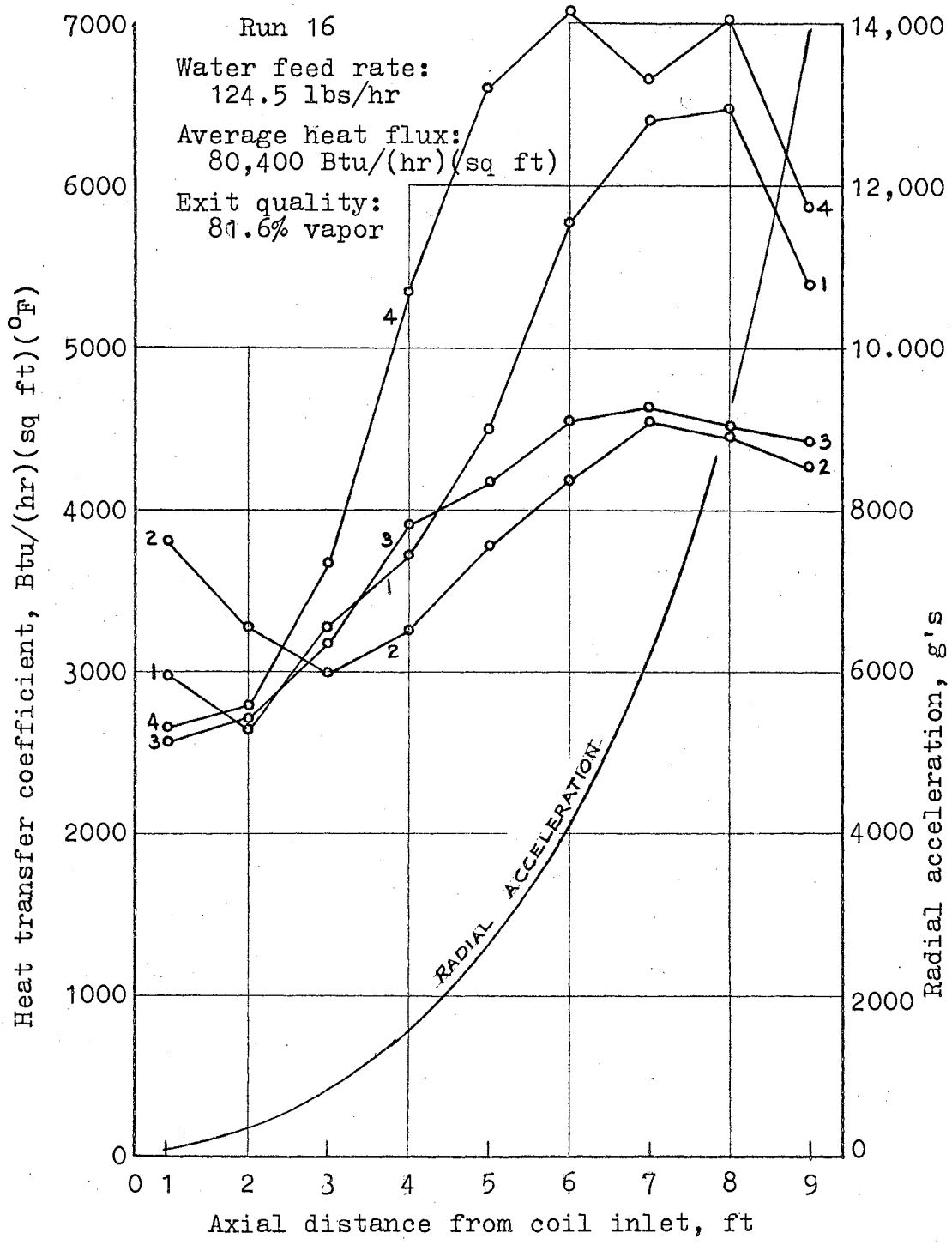

Fig. V-11 Saturated Boiling in Small Coil, High Heat Flux

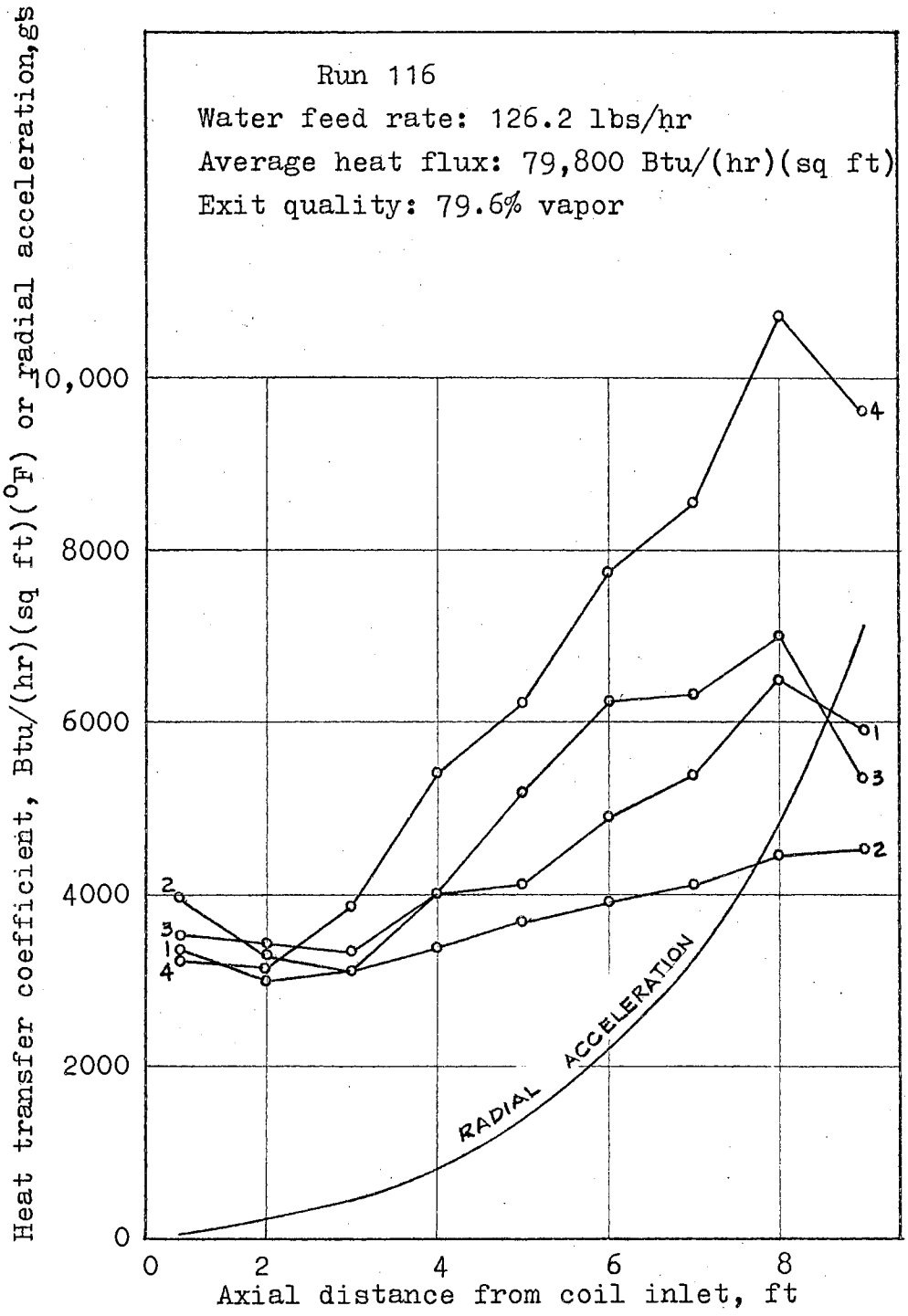

Fig. V-12 Saturated Boiling in Large Coil, High Heat Flux

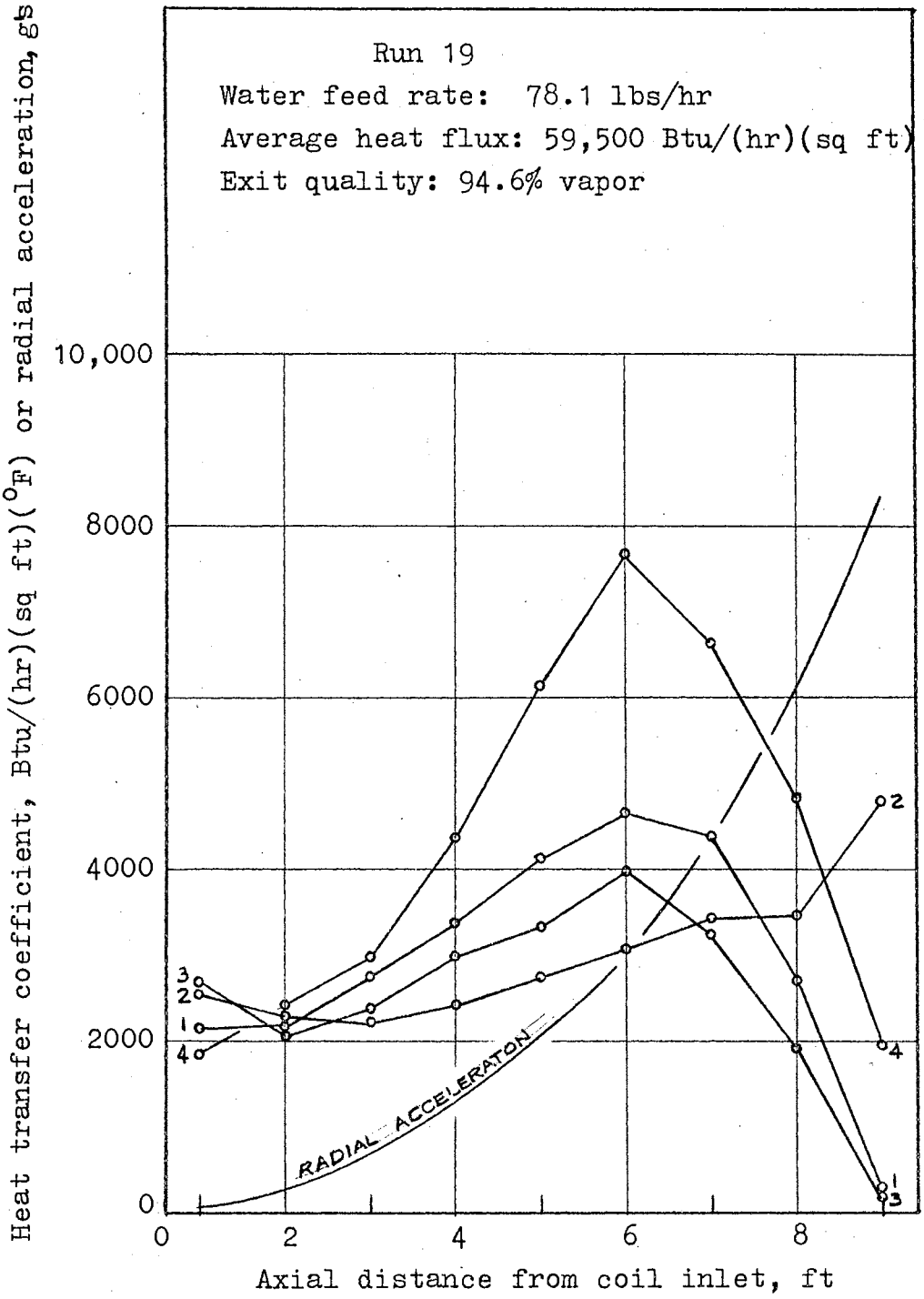

Fig. V-13 Saturated Boiling in Small Coil, High Exit Quality

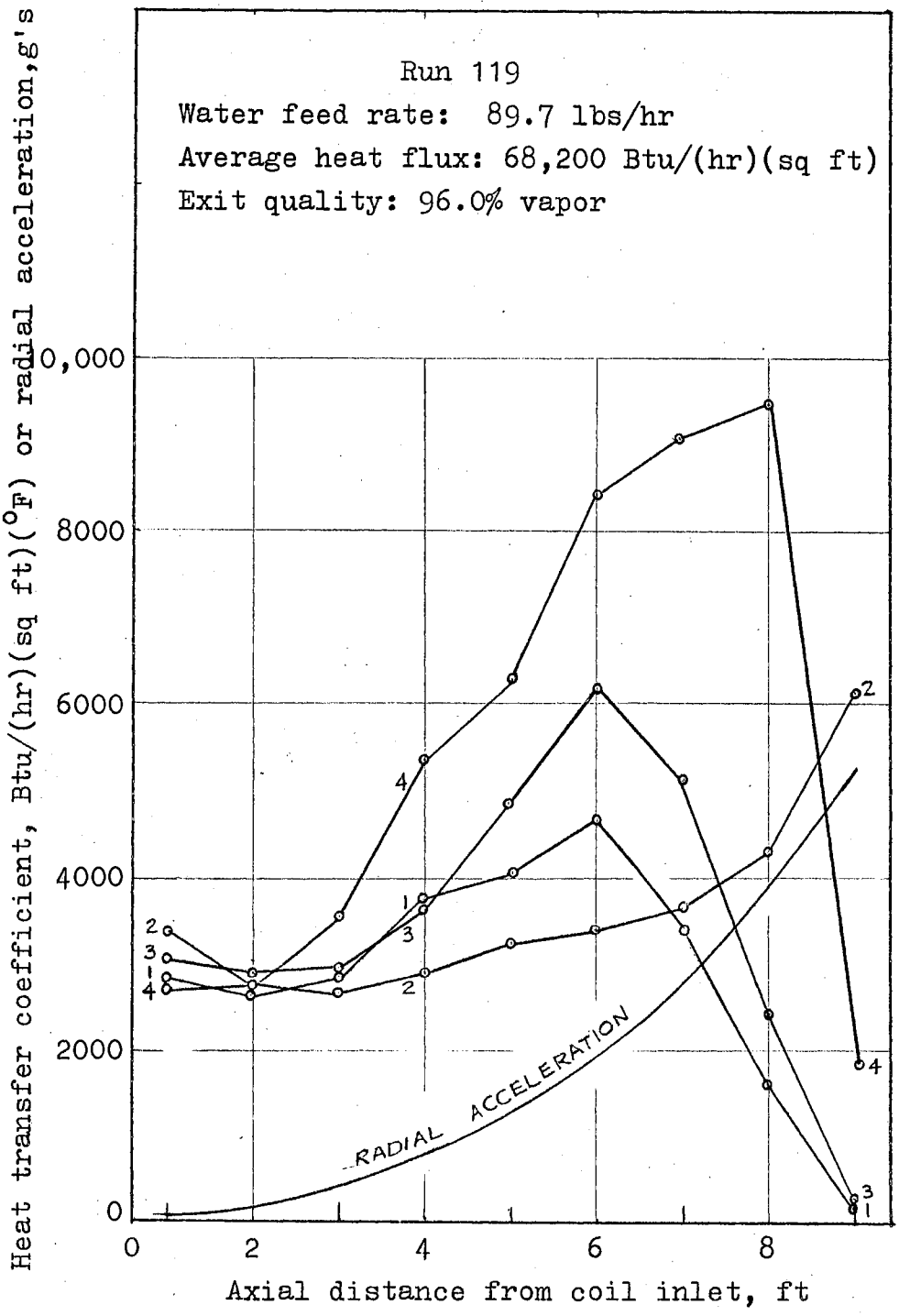

Fig. V-14 Saturated Boiling in Large Coil, High Exit Quality

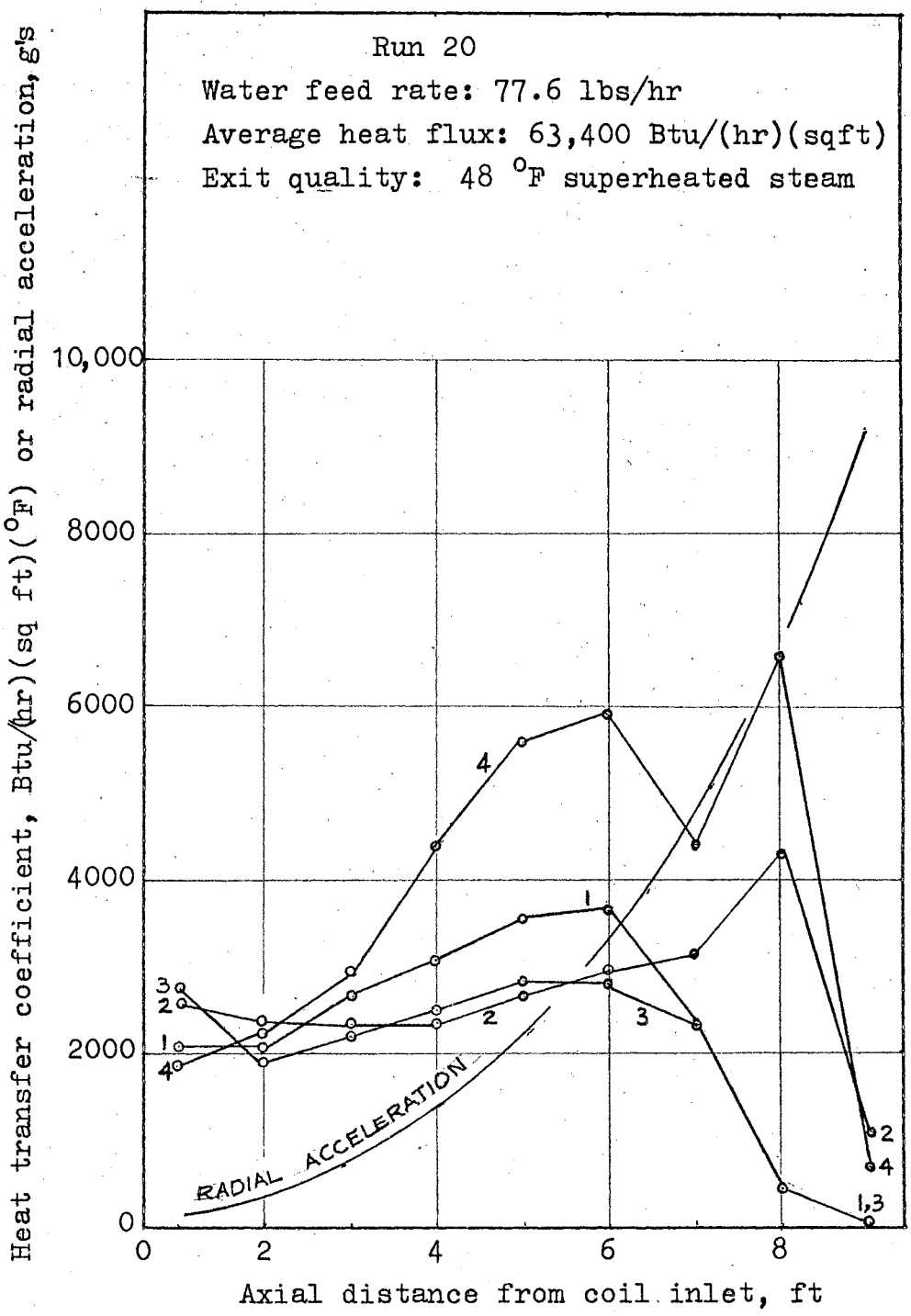

Fig. V-15 Saturated Boiling in Small Coil, Highest Exit Quality

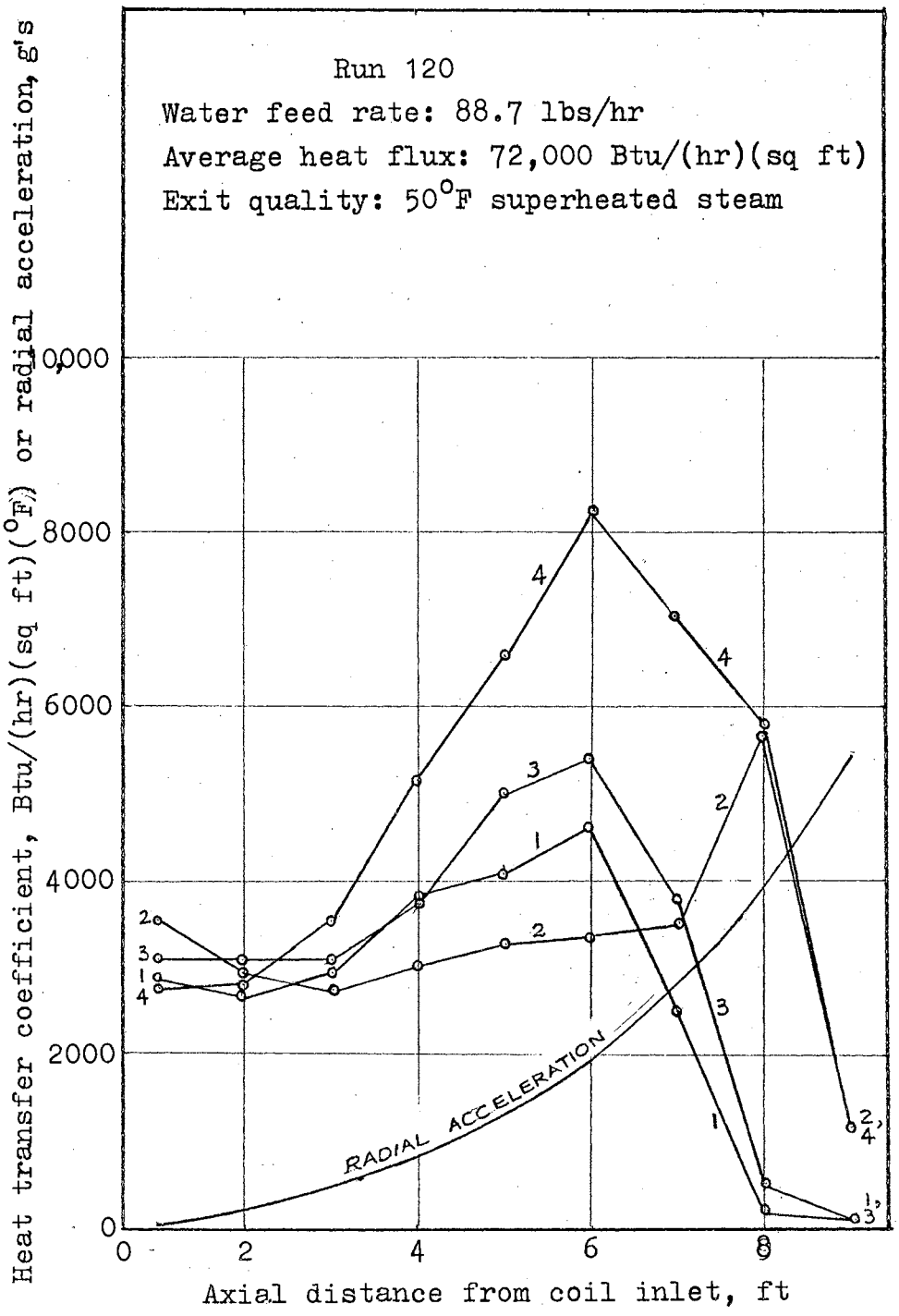

Fig. V-16 Saturated Boiling in Large Coil, Highest Exit Quality

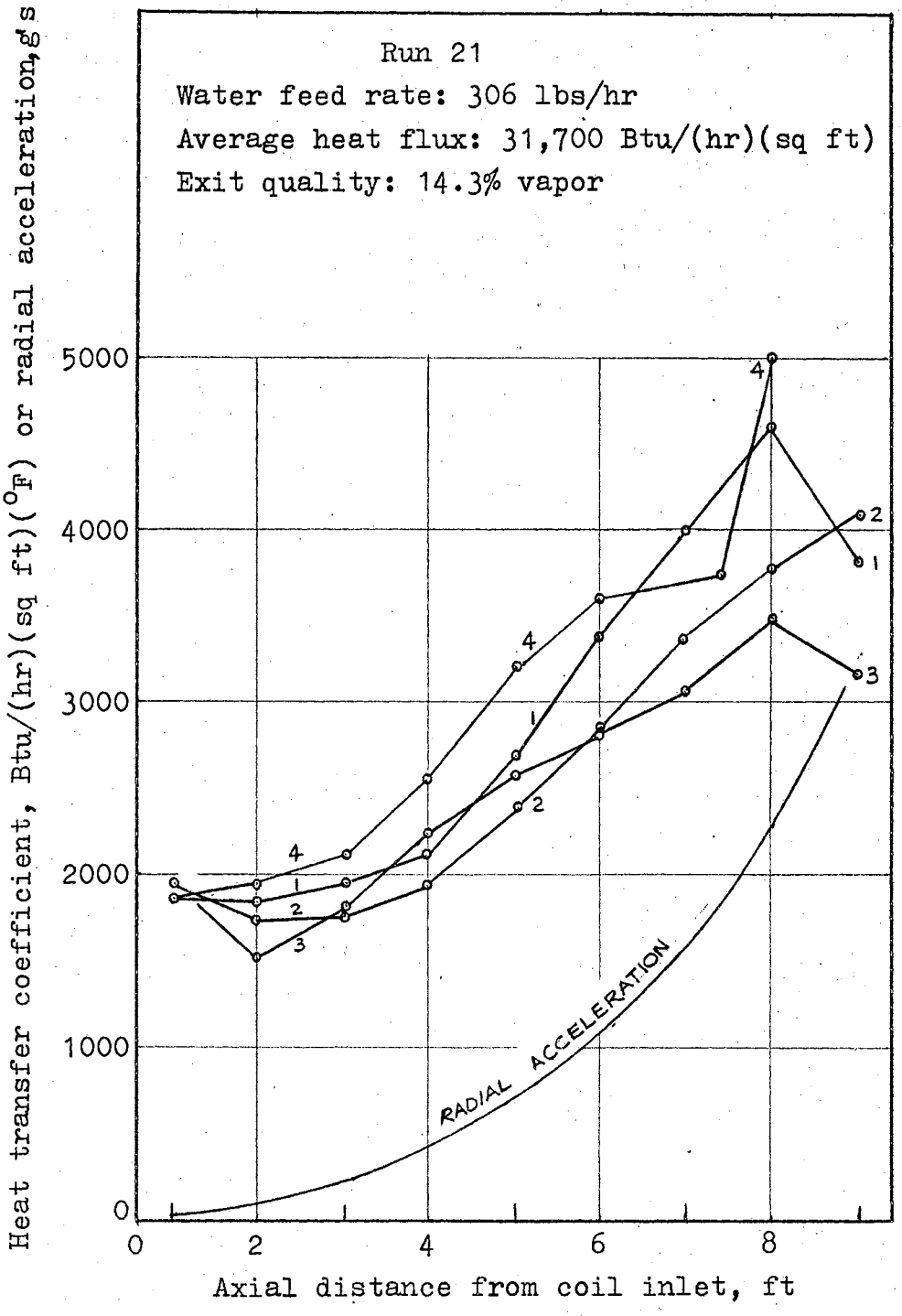

Fig. V-17 Saturated Boiling in Small Coil, Highest Feed Rate

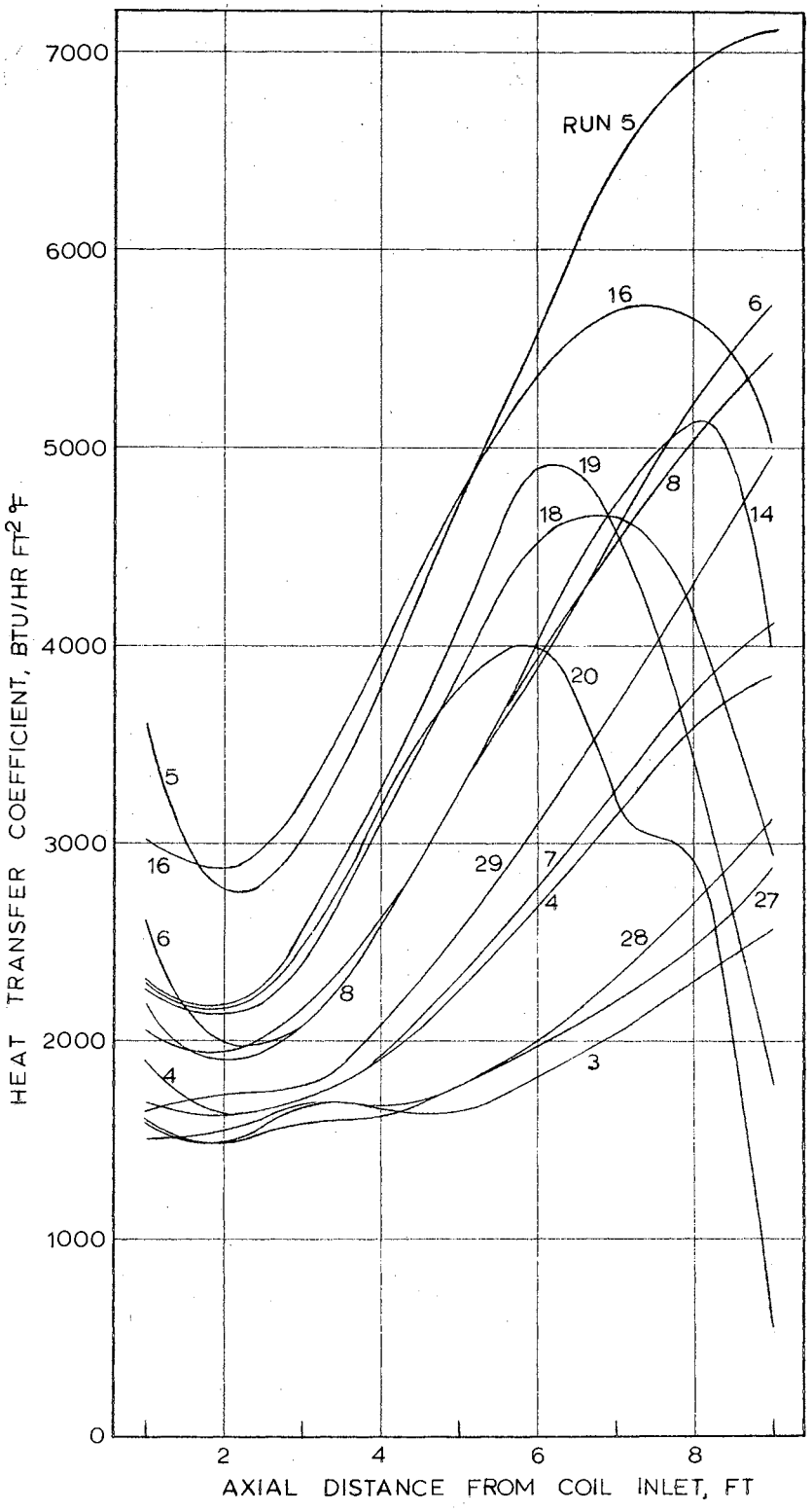

FIG. V-18 CIRCUMFERENTIAL AVERAGE HEAT TRANSFER COEFFICIENT FOR STABLE SATURATED BOILING RUNS, SMALL COIL.

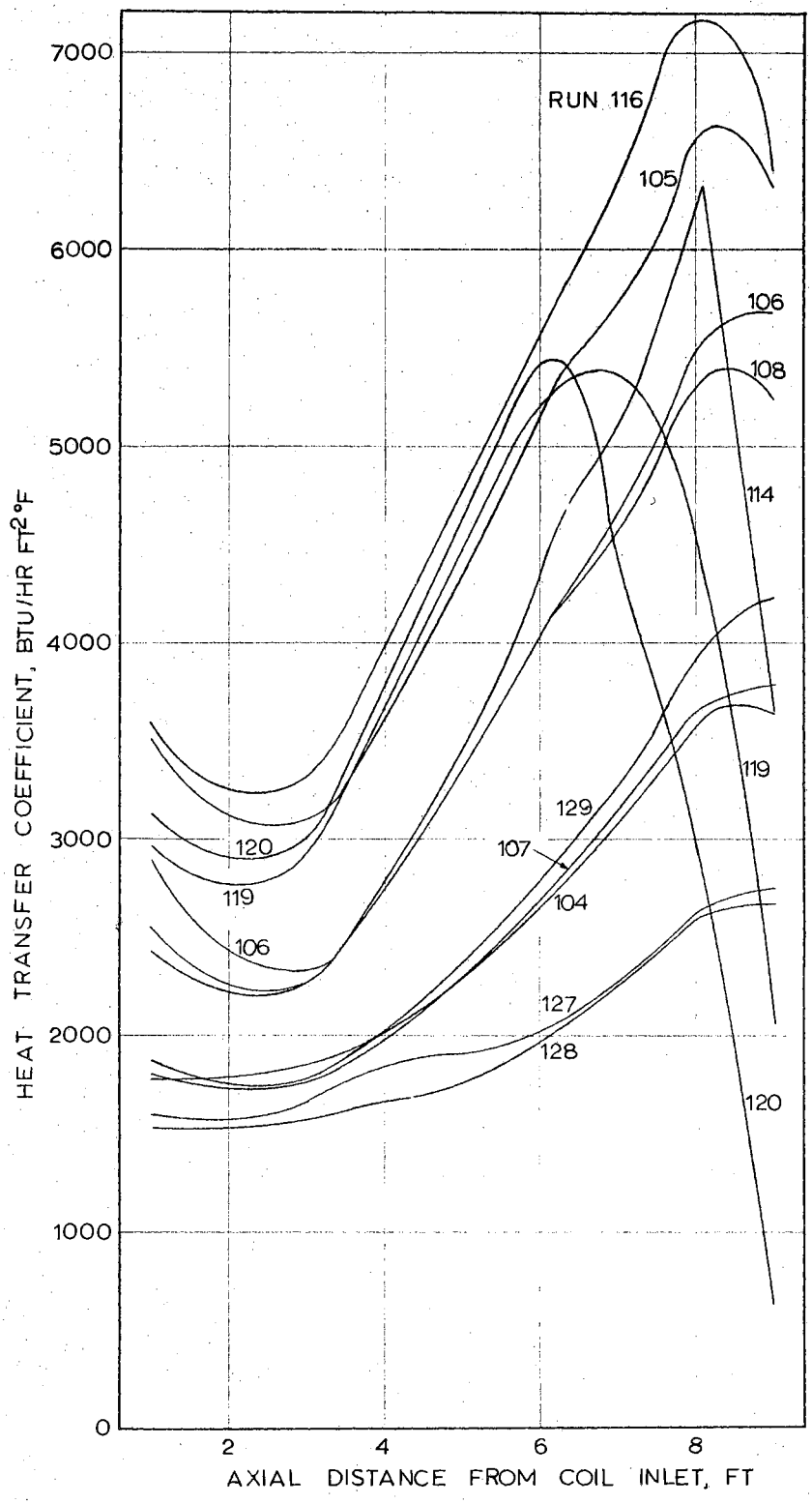

FIG. V-19 CIRCUMFERENTIAL AVERAGE HEAT TRANSFER COEFFICIENT FOR SATURATED BOILING RUNS, LARGE COIL.

nucleate boiling contribution superposed on the forced convective heat transfer.

As vaporization proceeds and greater turbulence is created, nucleate boiling is suppressed and the heat transfer mechanism becomes predominantly convective. There are evidences in support of this argument. For example, one can find conditions in different runs such that ΔT and the liquid flow rate are nearly the same, while the heat transfer coefficients are much higher at higher vapor rates (see Table V-1). In Table V-1 the vapor velocity and the liquid Re are both based on the total cross-sectional area of the tube.

TABLE V-1

EFFECT OF VAPOR VELOCITY ON

HEAT TRANSFER COEFFICIENT

Run	Thermocouple No.	ΔT ^{o}F	h Btu/hr ft^2 ^{o}F	Vapor Velocity ft/sec	Liquid Re
27	44	9.5	1790	55	5010
7	54	9.5	2940	104	4720
8	54	10.1	4320	143	4460
16	64	9.8	7070	232	3110

The values in Table V-1 all refer to the concave side--point 4.

Wattendorf (33) has shown that in single-phase flow of a fluid in a curved channel of rectangular cross-section, the shear stress on the concave wall (as seen by the fluid)

was higher than the convex wall. By analogy to momentum transfer, the resistance to heat transfer is expected to be less at the concave wall than the convex wall. In the author's experiments, the heat transfer coefficient for point 4 was the highest of all at moderate and high vapor velocities. Point 4 had the highest heat transfer coefficient in single-phase turbulent runs, also.

The heat transfer coefficient for all the points increases as more vaporization takes place until in the very high quality range (90-95 per cent) the coefficient for points 2 and 4 are still quite high, while for points 1 and 3 they diminish and approach the values of a gas coefficient (see Figs. V-13 through V-16). This is attributed to a liquid deficiency at points 1 and 3, but the hydrodynamics of the phenomenon are not clear.

As the vapor quality approaches 100 per cent, liquid deficiency also develops at points 2 and 4 and their coefficients drop rapidly also.

Pressure Drop

After all the temperature measurements were made, the thermocouples were removed from the coil and $\frac{1}{32}$-inch pressure taps were drilled at the top of the tube—point 1. One additional tap was drilled at location 94.

Pressure measurements at the coil inlet as well as the points along the coil were made under the conditions of

Runs 3, 4, 14, 27, 7, 8, 16, 28, 29, 6 and 5—all on the small coil. For the remainder of the runs for the small coil and all the runs for the large coil, only the inlet pressure was measured and the values along the coil were obtained by interpolating the results of the runs enumerated above. This procedure was thought satisfactory for computation of the local saturation temperature because the pressure drops for the two coils were not markedly different.

The conditions of heat flux and water feed rate were duplicated for each run and the pressures were measured with a mercury manometer. Correction was made for the height of water above the mercury.

The results of the pressure measurements for the small coil are shown in Fig. V-20 and their numerical values are listed in Appendix G.

The pressure at location 94 was always higher than 91, the difference being 0.4 psi in Run 5.

Stability

It was noticed that under some conditions of flow and heat flux the system pressure would oscillate in an orderly fashion (Fig. V-21). Under such conditions a surge of vapor and liquid would periodically discharge from the coil during approximately one third of the cycle. After the surge would subside, a rather steady stream, with a higher ratio of vapor to liquid, would flow for the remainder of the cycle. Runs 11, 12, 15, 10, 9, and 13 were of this nature.

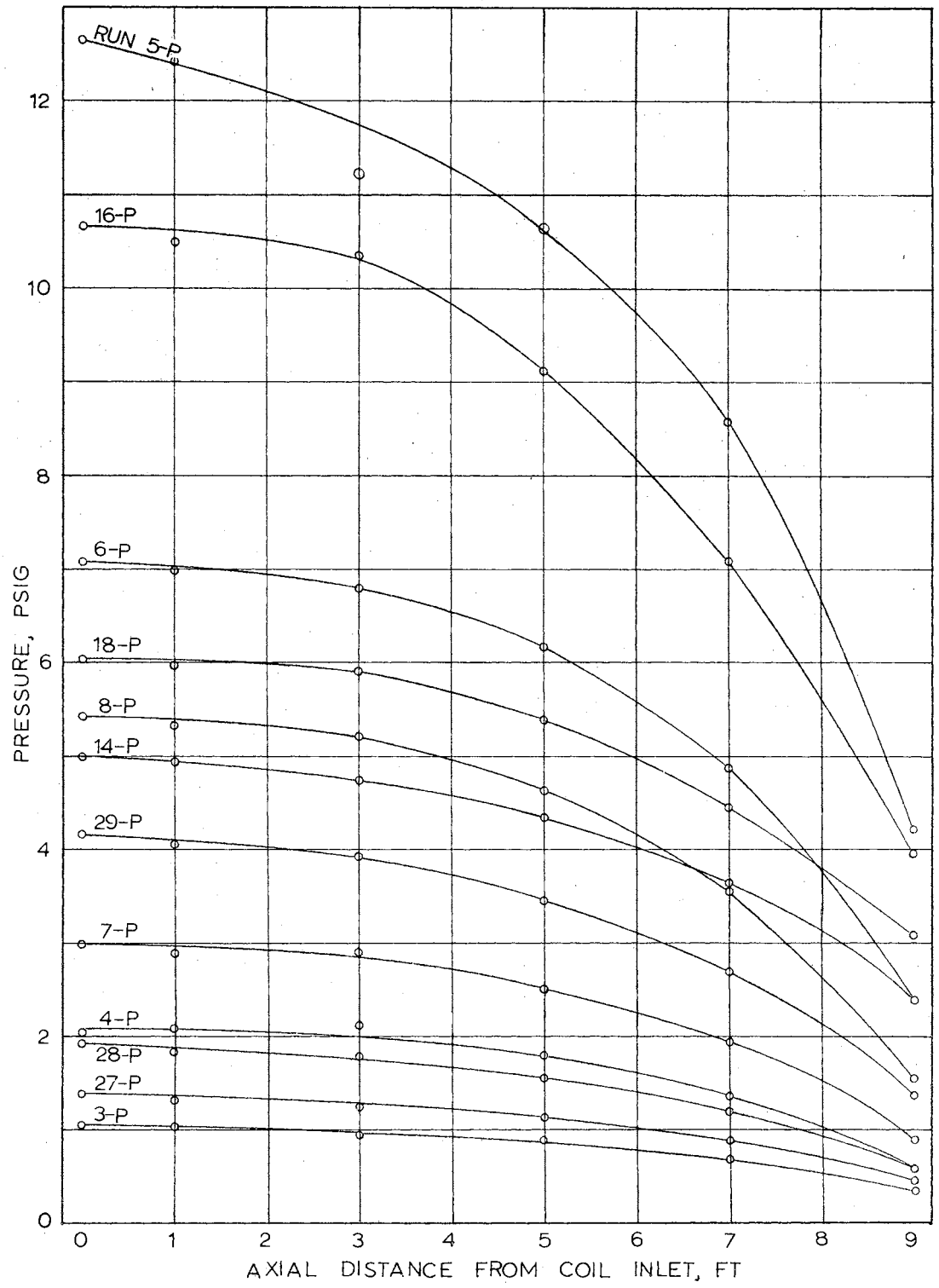

FIG. V-20. PRESSURE MEASUREMENTS FOR SMALL COIL.

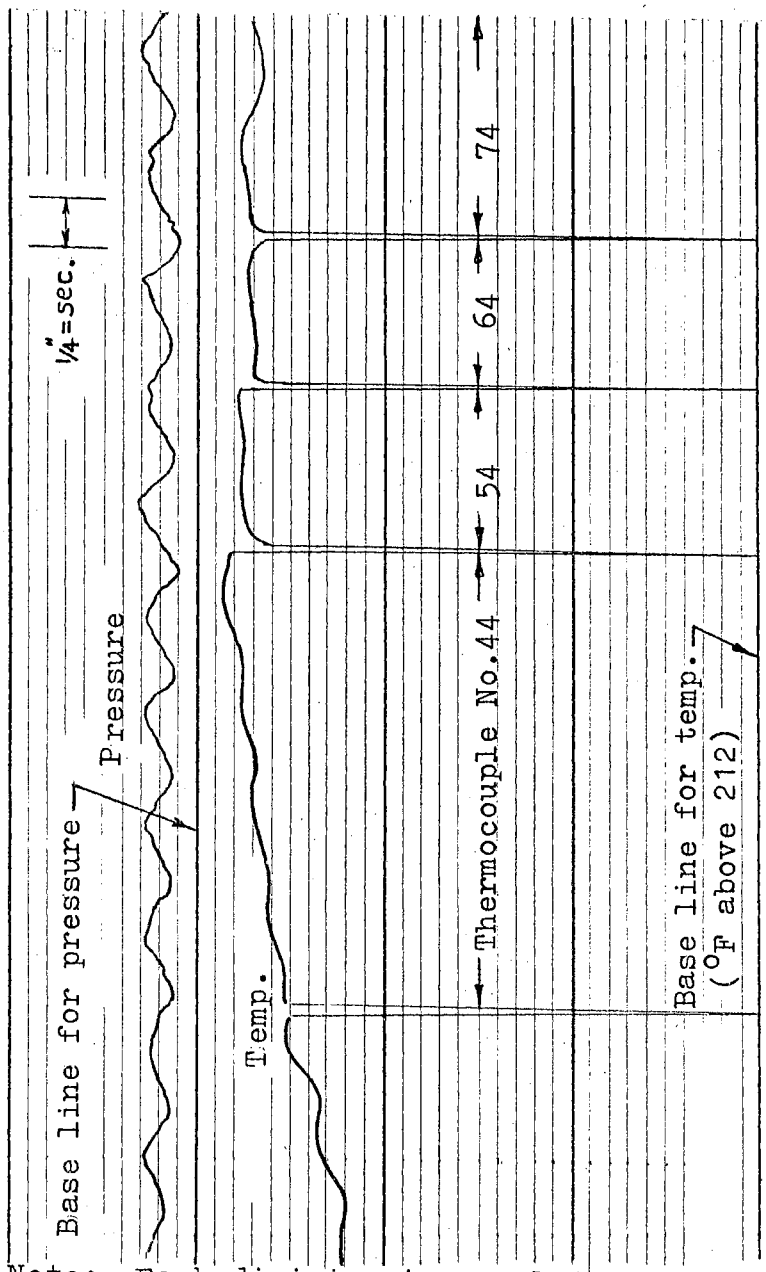

Note: Each division is equal to 1 psi or 1°F.

Run 13

Water feed rate: 47.0 lbs/hr

Average heat flux: 32,200 Btu/(hr)(sq ft)

Exit quality: 84.3% vapor

Fig. V-21 An Unstable Run

Since the water feed stream was throttled from a high pressure of about 50 psig, the pressure oscillations did not cause significant changes in the water flow rate as indicated by the rotameter. As the pressure oscillated, the temperatures would also oscillate, but with less regularity. The frequency and the extent of pressure oscillations for a few runs are listed in Table V-2.

TABLE V-2

FREQUENCY AND AMPLITUDE OF PRESSURE OSCILLATIONS

Run	Water Flow Rate lbs/hr	Average Heat Flux Btu/hr ft^2	Oscillation Period, sec	Range of Inlet Pressure Oscillation, psig
9	48.9	20,100	3.0	0.5 — 1.2
10	48.9	13,000	3.5	———
12	31.00	13,000	3.5	0.3 — 0.8
13	47.0	32,300	2.4	1.3 — 3.0
15	31.00	16,500	3.0	0.3 — 0.9

The variables influencing this phenomenon were not studied in detail. However, the following qualitative results may be stated:

1. Oscillations did not appear or disappear abruptly. Small-amplitude pressure oscillations could be discerned in some runs which did not cause perceptible temperature oscillations (see Fig. V-22).
2. At a given heat flux and inlet water temperature, increasing the flow rate increased the stability of the system.

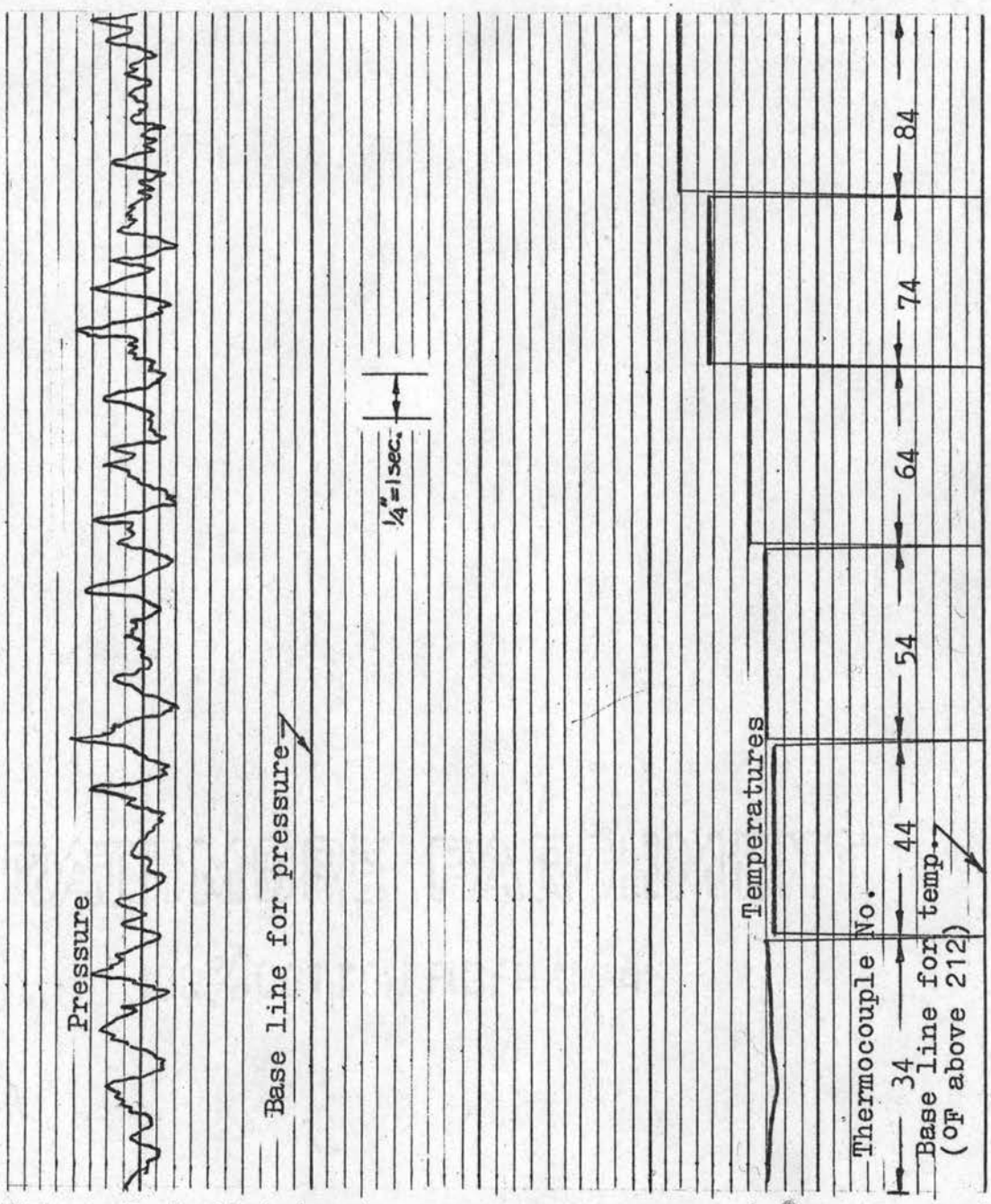

Note: Each division is equal to 1 psi or 3.3 °F.

Run 20 Water feed rate: 77.6 lbs/hr
Average heat flux: 63,400 Btu/(hr)(sq ft)
Exit quality: 48 °F superheated steam

Fig. V-22 A Nearly Stable Run

3. At a given flow rate and inlet water temperature, increasing the heat flux made the system less stable. For example, Runs 3, 4, and 14 were quite stable; Runs 18 and 19 had small pressure oscillations; and Run 20 was on the verge of instability.

4. At a given flow rate and heat flux, the less subcooling of the feed, the more stable the system was. However, if the feed stream contained some vapor, the system stability was affected adversely.

5. Some runs with small flow rates were unstable regardless of the feed temperature; such were Runs 11, 12, 15, 10, 9, and 13.

6. The smaller coil was more stable than the large coil; whereas Run 3 for the small coil was stable, a corresponding stable run could not be made with the large coil.

The conclusions in items 1, 2, 3, and 4 stated above are consistent with the observations of Gouse and Andrysiak (14) who made a detailed study of a loop containing a straight vertical boiling section.

As mentioned, Run 20 was close to being unstable. In this run the ratio of the heat flux to the water mass flux was 1.08 Btu/lb. However, at lower water rates the transition from stable to unstable would occur at a lower value of this ratio.

CHAPTER VI

CORRELATION AND DISCUSSION OF RESULTS

A theoretical analysis of heat transfer in two-phase flow is difficult due to the complex flow pattern, slip between vapor and liquid, the unknown condition at the vapor-liquid interface, and the formation of bubbles. Hence, a theoretical treatment of the subject has not yet been offered for any kind of geometry. In the following section previous correlations for straight tubes are presented first.

Correlation of Heat Transfer Data

Rohsenow (29) and others have suggested that forced convection heat transfer in subcooled or saturated boiling may be considered to be composed of two parts--a nucleate boiling component and a convective component, each of which may be correlated separately. Although this concept has been successfully applied to some problems, in general it is not clear how these two components should be combined, since the two mechanisms affect each other. Agitation suppresses bubble nucleation and growth, as can be seen readily by stirring a boiling pot of water. It has also been shown (1) that at high boiling rates, the effect of forced convection is substantially diminished.

Previous data on convective boiling in straight vertical tubes as well as the author's experiments suggest that at low vapor velocities a substantial nucleate boiling contribution is present, but at high velocities the convective mode overshadows the nucleate boiling.

No previous correlation for heat transfer to a two-phase flow in coils is available. Heat transfer to a two-phase flow in straight tubes has been correlated as a function of the Lockhart-Martinelli parameter by nearly all the authors in this field, some of them adding a nucleate boiling term. This parameter is defined as the square root of the ratio of the pressure gradient if the liquid phase alone flowed in the tube to the pressure gradient if the vapor phase flowed by itself

$$X = \sqrt{\frac{(dP/dL)_l}{(dP/dL)_g}} .$$

If both phases are turbulent, this parameter becomes

$$X_{tt} = \left(\frac{1 - x}{x}\right)^{0.9} \left(\frac{\rho_g}{\rho_l}\right)^{0.5} \left(\frac{\mu_l}{\mu_g}\right)^{0.1} .$$ Shi Ming Collier

The Lockhart-Martinelli parameter evolved from these authors' analysis and empirical correlation of isothermal two-phase, two-component pressure drop data in horizontal tubes (25). The gas phase in their experiments was always air and no acceleration pressure drop was present. The basic postulates of this analysis are that:

1. The pressure drop for the liquid phase is equal to that of the gas phase.

2. The volume occupied by the gas plus the volume occupied by the liquid must equal the total volume of the pipe.

In this correlation four flow regimes were recognized depending on whether the liquid or the vapor was in laminar or turbulent motion.

When adiabatic two-phase pressure drop data are plotted on the Lockhart-Martinelli correlation, liquid flow rate is seen to be a parameter within the overall correlation (see discussion at end of Lockhart and Martinelli's paper). This indicates that not all the variables influencing this phenomenon were taken into account. A second objection is that a plot of the actual pressure drop data reveal discontinuities which are undoubtedly associated with the change of flow regimes. The author also noticed this effect: when the water rate was decreased from 126 to 120 lbs/hr in Run 116, the total pressure drop of the system increased from 9.8 psi to 10.3 psi. In spite of these shortcomings, the Lockhart-Martinelli correlation remains the simplest and perhaps the best available today as attested by a critical evaluation by Dukler (9) of the various methods.

The extension of the Lockhart-Martinelli-type correlation to two-phase heat transfer is based on the analogy between heat and momentum transfer. In the two-phase pressure drop correlation, the modulus

$$\Phi_{gtt} = \sqrt{\frac{(dP/dL)_{TPF}}{(dP/dL)_g}}$$

is correlated against X_{tt}. In correlating two-phase heat-transfer data, in an analogous way, the ratio h_{TPF}/h_l is correlated with X_{tt}.

Dengler and Addoms' (8) heat transfer experiments were with two-phase flow of water in a steam-heated vertical tube at 8-40 psia. They correlated their data by

$$\frac{h_{TPF}}{h_l'} = 3.5 \left(\frac{1}{X_{tt}}\right)^{0.5}$$

where h_l' is the heat transfer coefficient if the total mixture were flowing in the tube as liquid. Where nucleate boiling was present, the right hand side of the equation was multiplied by a correction factor F. The correction factor F was empirically correlated as

$$F = 0.67 \left[(\Delta T - \Delta T') \left(\frac{dP}{dT_{sat}} \cdot \frac{d}{\sigma T_i}\right)\right]^{0.1}$$

Here ΔT is the wall minus saturation temperature, $\Delta T'$ is the temperature difference to initiate nucleate boiling under the prevailing flow velocity, $\frac{dP}{dT_{sat}}$ is the slope of vapor pressure vs. temperature curve at the saturation temperature. $\Delta T'$ was in turn given by the empirical formula

$$\Delta T' = 10 \, (V)^{0.3} .$$

The above correction is to be made only when $(\Delta T - \Delta T') > 0$.

Bennett et al. (2) studied heat transfer with two-phase flow of water in an internally heated annulus at pressures of 15-35 psia. Their correlation is given by

$$\frac{h_{TPF}}{h_l} = 0.64 \left(\frac{1}{X_{tt}}\right)^{0.74} \left(\frac{q}{A}\right)^{0.11} \qquad \text{(VI-1)}$$

Where nucleate boiling was present they added the value predicted by Rohsenow's equation (30).

Schrock and Grossman (31) proposed one equation to cover all cases:

$$\frac{h_{TPF}}{h_l} = 7.39 \times 10^3 \left[\frac{q/A}{Gh_{fg}} + 1.5 \times 10^{-4} \left(\frac{1}{X_{tt}}\right)^{0.66}\right]. \quad \text{(VI-2)}$$

Similar equations have been proposed by others.

Chen's correlation (4) is based on the assumption that the convective and the boiling components are always present, but the boiling component is suppressed more and more as turbulence increases. He correlates the convective component as a function of $\frac{1}{X_{tt}}$. The nucleate boiling component is evaluated from the Forster-Zuber equation (11), multiplied by a suppression factor S:

$$h_{mic} = 0.00122 \frac{k_l^{0.79} C_{pl}^{0.45} \rho_l^{0.49} g_c^{0.25}}{\sigma^{0.5} \mu_l^{0.29} h_{fg}^{0.24} \rho_v^{0.24}} \quad \text{(VI-3)}$$

$$(\Delta T)^{0.24} (\Delta P)^{0.75} S ,$$

where h_{mic} is the nucleate boiling component of the heat transfer coefficient, ΔP is the difference in vapor pressure, in pounds per square foot, corresponding to ΔT, and g_c has the value of 4.17×10^8 lb_m ft/(lb_f)(hr^2); the other symbols and their units are defined in the Nomenclature. The suppression factor S is in turn given as a function of a so-called two-phase Reynolds number, $\left[\frac{h_{conv}}{h_l}\right]^{1.25} Re_l$. This correlation is based on several

sets of data with water and organic compounds obtained by various investigators; it is the best available now.

To correlate the heat transfer data from the coils, it appeared that X_{tt} was still the appropriate parameter to choose. Since X_{tt} expresses the ratio of two pressure gradients, the geometrical consideration disappears.

Inherent in the Lockhart-Martinelli analysis is a model of annular flow of liquid with a vapor core. In view of the strong radial acceleration created in a coil, it is unlikely that an appreciable fraction of the liquid can be entrained in the vapor core. Although the shear exerted by the vapor on the liquid tends to entrain the liquid into the turbulent eddies, the liquid droplets are quickly deposited back on the wall.

Based on the experimental measurements of the heat transfer coefficient around the tube it was evident that a liquid film exists all around the tube. This behavior was attributed to the secondary flow.

The secondary flow is caused by the action of the centrifugal force when a fluid flows in a curved path. The liquid near the center of the tube has the highest velocity and is most strongly acted on by the centrifugal force. This force drives the fluid from the center to the outer wall of the tube. This in turn induces a motion from the outer wall around the tube and back to the center (see Fig. I-2). The net result is a pair of symmetrical re-circulation patterns superposed on the main flow.

When a river flows in a curved path, this phenomenon accounts for the increased erosion of the banks of the river. Secondary flow is also responsible for the higher friction in curved pipes compared to straight pipes.

It is well known that the hydraulic resistance of a pipe bend is equivalent to several feet of straight pipe; and the sharper the bend, the higher the resistance. However, it is experimentally proved that only a small fraction of the pressure drop attributed to a bend occurs in the bend itself; most of the drop takes place in the straight section of the pipe following the bend (7). This is because the secondary flow persists after the bend and the energy associated with it is gradually dissipated by the viscous forces in the straight tube following the bend; and the sharper the bend, the stronger the secondary flow and the higher the energy dissipation after the bend.

The secondary flow develops a higher pressure at the concave side of the tube compared to the other points. It is noticed in Run 5-P that the pressure at location 94 was 0.4 psi larger than that of location 91. This pressure difference is equivalent to a velocity head of 278 ft/sec for the vapor at the existing conditions.

The investigations of the pressure drop and heat transfer in coils reported in the literature have not contributed materially to the understanding of the secondary flow. Theoretical treatments of the secondary flow have dealt with the laminar and the inviscid case (see e. g. Hawthorne (15)).

Therefore, an adequate knowledge of the subject has not yet been achieved.

Regarding heat transfer in two-phase flow in a helix, the following mechanism is postulated: A secondary flow exists in the vapor core of the two-phase flow. This secondary flow exerts a drag on the liquid and causes it to flow from the outer to the inner wall of the tube, constantly replenishing the losses due to evaporation and entrainment. Liquid on the wall is subject to small radial acceleration effects because its axial velocity is very small. The vapor, being surrounded by a liquid film, is isothermal at its saturation temperature. At high qualities, when the continuous liquid film finally breaks, the remaining liquid is concentrated at the stagnation points of the secondary flow (points 2 and 4) and the heat transfer coefficient at other points decreases to the pure vapor coefficient.

For the purpose of correlation, only the circumferential average heat transfer coefficient was considered. Of the four X's associated with the four flow regimes, X_{tt} was felt to be suitable even when the liquid Reynolds number was below the critical value. For two-phase flow in a straight tube the critical Reynolds number was arbitrarily set at 2000 by Lockhart and Martinelli. Since the liquid is not flowing by itself, this number loses the significance that it has in single-phase flow, as the authors readily admit. Furthermore, in a coil the transition from laminar

to turbulent is made smoothly and the difference between the two regimes is less pronounced than in a straight tube. Lastly, the Lockhart-Martinelli curve for the case of viscous liquid-turbulent gas regime does not differ radically from the curve for the case when both phases are turbulent. It should be pointed out that the Reynolds number for each phase is based on the total cross-sectional area of the tube.

Fig. VI-1 is the correlation of h_{TPF}/h_{lc} as a function of X_{tt} for the small coil and Fig. VI-2 for the large coil. h_{lc} is the value of the heat transfer coefficient if the liquid phase alone were flowing in the coil; it was calculated from Seban and McLaughlin's correlation for turbulent flow heat transfer in a coil, namely

$$h_{lc} = 0.023\ Re^{0.8}\ Pr^{0.4}\ [Re^{0.05}\ (\frac{d}{D})^{0.1}]\ \frac{k_l}{d}\ . \qquad (VI-4)$$

This procedure implies that the resistance to heat transfer in two-phase flow is essentially in the liquid film. The physical properties of the liquid evaluated at the saturation temperature were used to calculate h_{lc}. In each case the appropriate value of coil diameter was used in the above equation.

The correlation curve for the large coil is nearly the same as that of the small coil.

Correlation of Pressure Drop Data

The Lockhart-Martinelli method (25) was used, with a modification, to correlate the pressure drop data, namely,

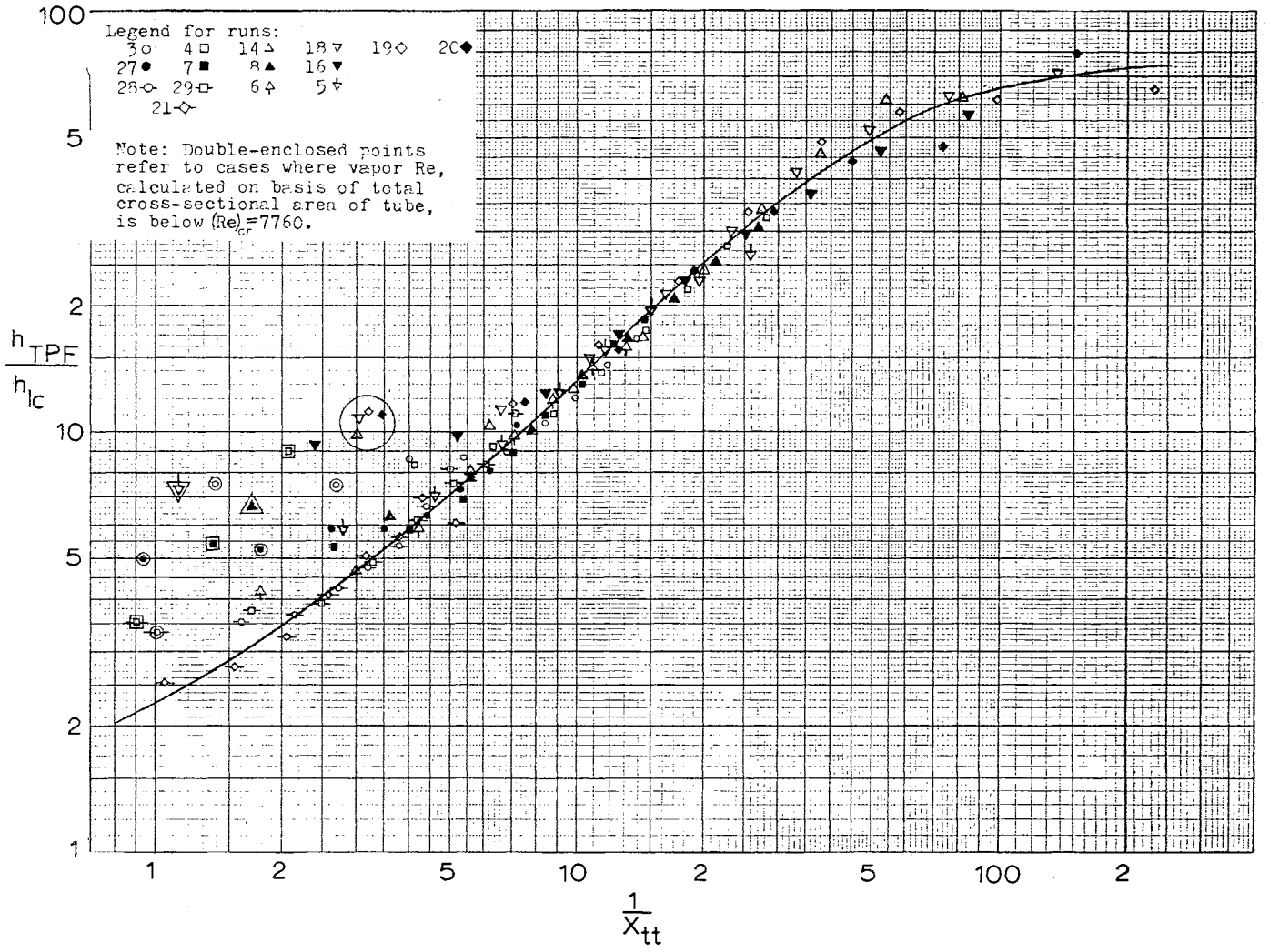

FIG. VI-1. CORRELATION OF DATA OF HEAT TRANSFER IN TWO-PHASE FLOW, SMALL COIL.

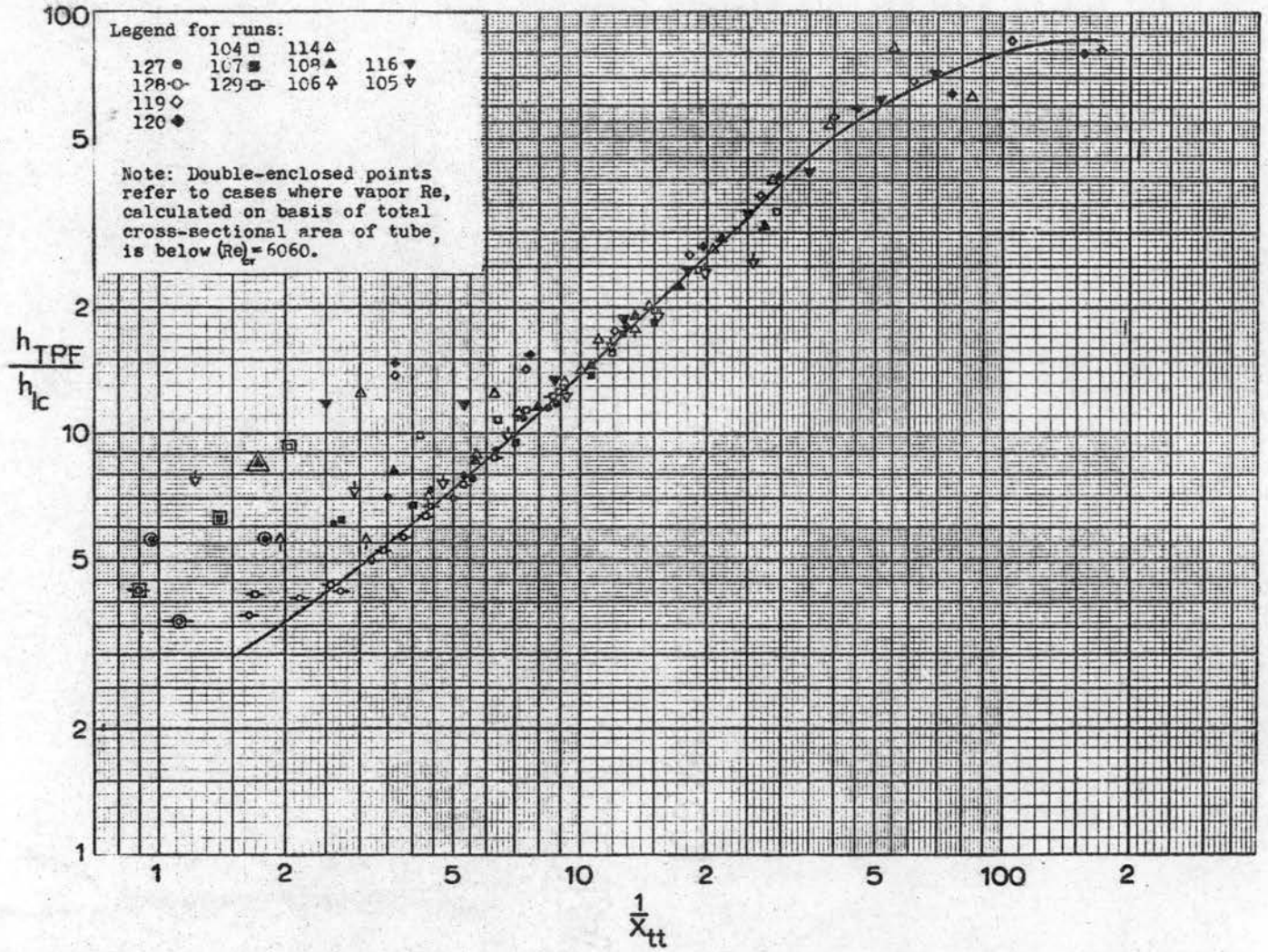

FIG. VI-2. CORRELATION OF DATA OF HEAT TRANSFER IN TWO-PHASE FLOW, LARGE COIL.

$\phi_{gtt} = \sqrt{\frac{(dP/dL)_{TPF}}{(dP/dL)_g}}$ was plotted against $X_{tt} = \sqrt{\frac{(dP/dL)_l}{(dP/dL)_g}}$.

The measured values of the pressure drop were the sum of the friction pressure drop, the acceleration pressure drop, and the elevation pressure drop. The elevation pressure drop could be approximated by the static head exerted by a column of fluid with a density equal to the average density of the vapor-liquid mixture in the coil. Based on the liquid hold-up data of Rippel et al. (27), it was concluded that the hydrostatic head was usually less than 1 per cent of the total pressure drop; therefore, it was neglected.

In order to calculate the acceleration pressure drop, it was assumed that the liquid flows in an annular film. The volume fraction of the tube filled with liquid, R_l, was obtained from the experimental data in (27). Knowing R_l and the liquid flow rate, the average liquid velocity in the film can be determined. The acceleration pressure drop, ΔP_a, was calculated from

$$\Delta P_a = \frac{G^2}{g_c}\left[\frac{(1-x)^2}{R_l} + \frac{x^2}{(1-R_l)}\,\frac{\rho_l}{\rho_g} - 1\right]\frac{1}{\rho_l} \qquad \text{(VI-5)}$$

which is derived rigorously from a momentum balance between the liquid feed stream and the product stream composed of liquid and vapor.

The friction pressure drop, obtained by subtracting the acceleration pressure drop from the total pressure drop, was then plotted against coil length and the slope of the curve,

$\left(\frac{dP}{dL}\right)_{TPF}$, was determined graphically.

In the Lockhart-Martinelli correlation, $(dP/dL)_g$ represents the calculated pressure gradient if the gas phase alone flowed in a straight tube. This is modified here such that $(dP/dL)_g$ is taken as the pressure gradient if the vapor phase alone flowed in the coil under consideration.

The friction factor for the turbulent flow of fluids in a coil is given by Ito (17):

$$\frac{f}{f_s} = Re^{0.05} \left(\frac{d}{D}\right)^{0.1} \qquad \text{(VI-4)}$$

where f is the friction factor for the coil and f_s is the friction factor for a straight tube. For a smooth straight tube f_s is calculated from the Blasius' equation, valid in the range of $2.1 \times 10^3 < Re < 10^5$

$$f_s = .0791\ Re^{-.25} \qquad \text{(VI-5)}$$

f_s is the Fanning friction factor so that

$$\frac{dP}{dL} = \frac{2 f_s \rho U_\infty^2}{g_c\ d} \qquad \text{(VI-6)}$$

U_∞ is the free stream velocity. Here, U_∞ was approximated by the mean vapor velocity based on the total cross-sectional area of the tube. Therefore,

$$\left(\frac{dP}{dL}\right)_g = \frac{2 \times .0791\ Re^{-0.2} \left(\frac{d}{D}\right)^{0.1} \rho_g\ V_g^2}{g_c\ d} \qquad \text{(VI-7)}$$

The results of plotting ϕ_{gtt} vs X_{tt} for Runs 5, 6, 8, 14, 16, and 29 are shown in Fig. VI-3. The solid line is the Lockhart-Martinelli correlation for turbulent gas—turbulent liquid system in straight horizontal tubes.

The results of the small coil data fall along the

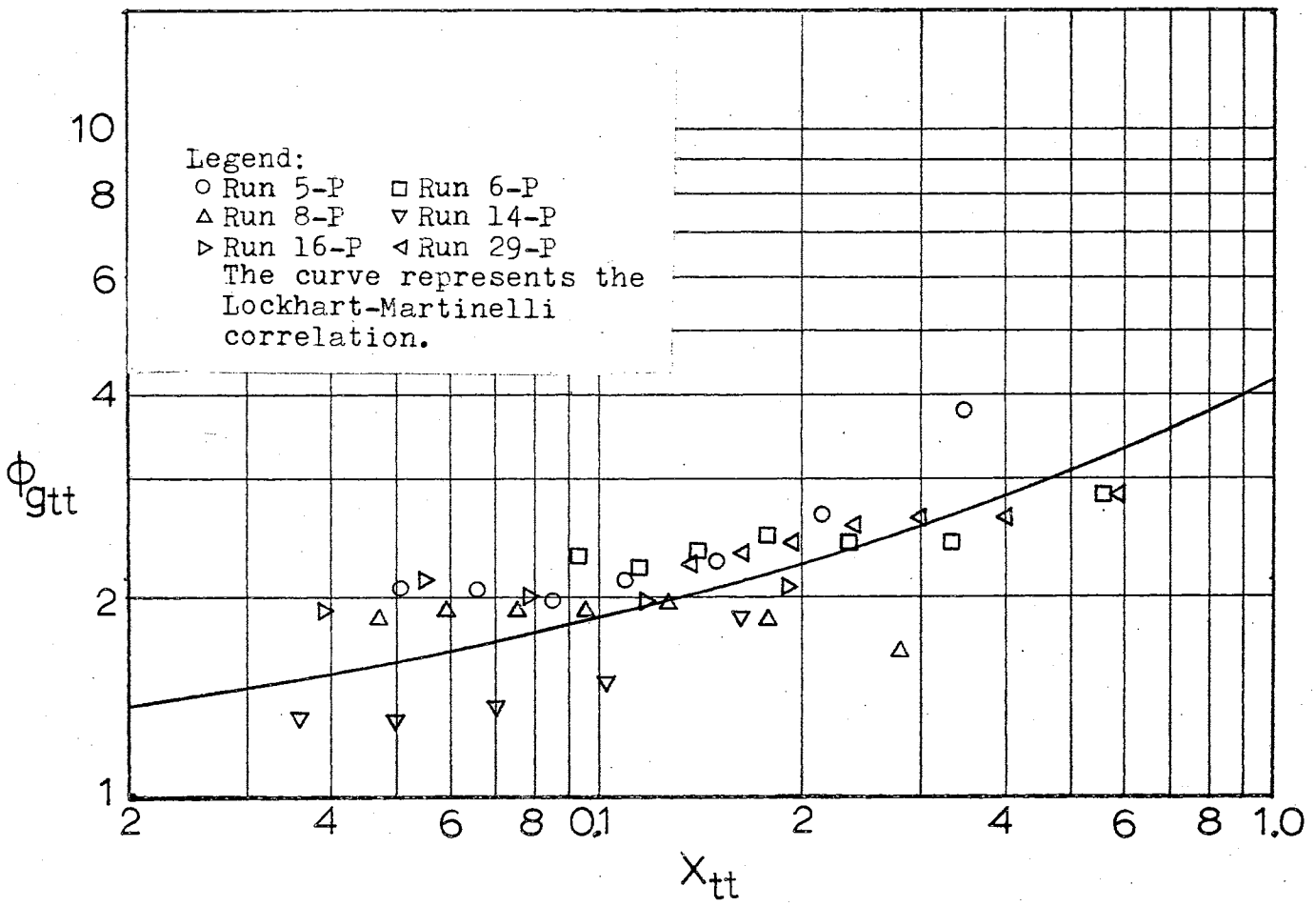

Fig. VI-3 Pressure Drop Correlation For Small Coil

solid line. In the case of the large coil, only the inlet pressure was measured in each run; therefore no correlation could be attempted. The values and their scattering are comparable to the coil results in (27) and also comparable to the straight tube results reported in the literature.

Discussion of Results

In the low quality range, the high values of h_{TPF}/h_{lc} indicate the presence of nucleate boiling (see Figs. VI-1 and VI-2). An improved correlation may be obtained by including a nucleate boiling component which would be progressively suppressed as the liquid Reynolds number or the vapor quality is increased, as successfully applied by Chen (4) in the correlation of two-phase heat transfer in straight tubes. However, this was not done here since the primary purpose of this work was to gain a general understanding of the problem. As such, the values obtained from the curve in the low quality range will be conservative for design purposes.

In the medium quality range, the correlation is good. However, the data scatter in the high quality range. This is due to the inherent difficulty of obtaining sufficiently accurate data in the very high quality range, e.g., one per cent error in the input power or liquid flow rate causes 18 per cent error in the calculated value of X_{tt} when the quality is 95 per cent and correspondingly higher errors at higher quality. Also, in this quality range the temperature

variation around the tube is relatively large and four temperature readings are not sufficient to accurately describe the temperature profile around the tube. Consequently, the accuracy of the calculated radial heat flux diminishes (see Appendix H for detailed discussion of experimental errors).

The data for all liquid flow rates fall along the same line, and no distinction can be made between a laminar and a turbulent liquid phase. Even though the calculated values for h_{lc} are based on turbulent flow of a liquid in a coil, it was found that the form of Eqn. (VI-4) was still a satisfactory non-dimensionalizing parameter for all the liquid Reynolds numbers encountered, some of which were close to 1000.

Since only two coil diameters were investigated, no definite statement can be made regarding the effect of this variable on heat transfer. In Eqn. (VI-4) the effect of coil diameter appears in the form of $(d/D)^{0.1}$, the value of which is only 7.6 per cent greater for the small coil compared to the large coil. In view of the fact that the results of the two coils, plotted in the manner described, fall essentially along the same line, it may be stated that, in the range of coil diameters investigated, the effect of the ratio of tube to coil diameter on the heat transfer coefficient in two-phase flow is not basically different from its effect in single-phase turbulent flow.

No claim can be made concerning the extension of this

correlation to high pressures or to other liquids.

Comparing the results found here with the heat transfer correlations of two-phase flow in straight tubes, it was noticed that Chen's correlation predicted about 15 per cent higher coefficients at low qualities and 15 per cent lower coefficients at high qualities. At very high qualities where all the sides of the tube are not wetted to the same extent, Chen's correlation predicts coefficients which are as much as three times the measured values.

Dengler and Addoms' correlation predicts values which are, on the average, only 10 per cent less than the author's experimental values in the low and medium quality ranges. However at qualities above 70 per cent it predicts values which are 30 to 50 per cent too high until at 90 per cent quality its predicted values are several times the author's measured values. It should be noted that the highest vapor quality in the data used in Dengler and Addoms' correlation, as well as Chen's correlation, was 71 per cent.

The values predicted by Schrock and Grossman are about 20 per cent too low in the low quality range and about 60 per cent below the measured values in the high quality range.

The most significant feature of the helix is that it delays the transition from a wetted wall to a dry wall condition. In the experiments of Dengler and Addoms (8) on boiling water in a 1-inch I.D. steam-heated straight vertical tube this transition occurred at a vapor quality of about 80 per cent when the flow rate was 240 lbs/hr. They observed

that, at a given flow rate, this transition always occurred at the same vapor quality. The transition vapor quality was higher at a low flow rate than at high.

In the experiments of Woods (35) on boiling water in a standard 1-inch, steam-heated, horizontal copper pipe the transition occurred at vapor qualities of 65-85 per cent.

No criterion has been established for the transition from a wet wall to a dry wall condition. In a heat flux-controlled system the transition is also a function of the heat flux.

In both coils the transition appears to occur at 85-90 per cent vapor quality at points 1 and 3, while occurring at 98-100 per cent vapor quality at points 2 and 4 (Runs 20 and 21). It should be emphasized that these values apply only to the conditions of these two tests and cannot be generalized. Nevertheless, they reveal qualitatively this useful feature of the helix.

CHAPTER VII

CONCLUSIONS AND RECOMMENDATIONS

Boiling heat transfer was studied in two helical coils with diameters of 9.86 and 20.57 inches made of 0.4924-inch bore Inconel tubing. The fluid studied was water and the system outlet pressure was approximately atmospheric. Two-phase heat transfer and pressure drop were empirically correlated as a function of the Lockhart-Martinelli parameter. Single-phase heat transfer data were compared with the existing correlations. Subcooled boiling data were presented without correlation. Observations on the system stability were made.

The heat transfer coefficient is in general, quite high on all sides of the tube, although the heat transfer coefficient on the concave side of the tube is usually higher than the convex side. It is postulated that the secondary flow (see Fig. I-2) is responsible for distributing the liquid around the tube.

At qualities above 80 per cent the heat transfer coefficient at the concave and convex sides are both high indicating that they remain wetted by the liquid, while the heat transfer coefficient at the top and the bottom of the tube decrease gradually until at about 95 per cent quality

they approach the value expected of a gas. The accuracy of the values calculated in the high quality range is not as good as the accuracy of those in the low and medium quality range.

The highest quality at which measurements were made was 99.1 per cent vapor, although the exit vapor was 50 ^{o}F superheated steam. Even at this quality, both the concave and the convex sides of the tube were partially wetted. The common feature of the points 2 and 4 (see Fig. III-4) is that both are stagnation points. However, a completely satisfactory explanation could not be offered for the above observation. An adequate understanding of the secondary flow phenomenon has not yet been achieved.

Over most of the quality region the controlling heat transfer mode is convection, but a nucleate boiling component is present at the low qualities. The nucleate boiling is suppressed as turbulence increases.

To study the high quality range, a system should be devised where a high quality mixture is synthesized and introduced to the coil, thereby determining the quality more accurately. Also, numerous thermocouples—as many as 12—around the periphery are needed to determine the circumferential temperature profile on the tube at high qualities.

Choosing a thin wall for the tube has the apparent advantage of smaller circumferential conduction. It also has the disadvantage of steeper circumferential temperature

gradients. Due to these opposite effects on accuracy, the overall results may not be substantially more accurate for a thin compared to a thick wall.

Generally, the experiments reported here were under the condition of high vapor velocity and radial acceleration. The extension of the present correlation to high pressures where the vapor velocity and radial acceleration are substantially lower is not recommended. This remains an area of future research. Also, the important phenomenon of departure from nucleate boiling remains to be studied.

The helical coil should be considered in applications where the total liquid stream is to be vaporized. The transition from a wetted wall to a dry wall occurs at considerably higher qualities compared to a straight tube.

The coil is a suitable device for boiling in the absence of gravity. It also has attractive features as a chemical reactor where large volumes of vapor react with a liquid accompanied by a high heat of reaction such as chlorination reactions. It provides for very efficient contact and excellent heat transfer. The secondary flow destroys the radial concentration gradient, making it behave close to a plug flow reactor.

A SELECTED BIBLIOGRAPHY

(1) Beecher, Norman. (unpublished S.M. thesis in Chemical Engineering, Massachusetts Institute of Technology, Cambridge, Mass. 1948).
see also:
McAdams, W. H. Heat Transmission, 3rd ed., McGraw-Hill, (1954) p. 378.

(2) Bennett, J. A. R. et al. Trans. Inst. Chem. Engrs. (London), 39, (1961) pp. 113-26.

(3) Carver, J. R., C. R. Kakarala, and J. S. Slotnik. "Heat Transfer in Coiled Tubes With Two-Phase Flow." Atomic Energy Commission Document TID 20983, (1964).

(4) Chen, J. C. "A Correlation For Boiling Heat Transfer to Saturated Fluids in Convective Flow." Amer. Soc. Mech. Engrs. Paper 63-HT-34 (1963)

(5) Collier, J. G., G. B. Wallis, and N. Zuber. "Two-Phase Flow and Heat Transfer," Notes of Summer Course, June 27-July 9 (1965), Dartmouth College, Hanover, N. H.

(6) Costello, C. P. and J. M. Adams. "The Interralation of Geometry, Orientation, and Acceleration in the Peak Heat Flux Problem." Amer. Inst. Chem. Engrs. Vol. 9, No. 5, (1963) 663.

(7) Daugherty, R. L. and J. B. Franzini. Fluid Mechanics With Engineering Applications, 6th ed., McGraw-Hill, New York, N. Y. (1965) p. 228.

(8) Dengler, C. E. and J. N. Addoms. "Heat Transfer Mechanism for Vaporization of Water in a Vertical Tube." Chem. Engr. Prog. Symp. Series, 52, No. 18, (1956) 95.

(9) Dukler, A. E. et al. A. I. Ch. E. Journal, 10, No. 1, (January 1964) 38-51.

(10) Eckert, E. R. G. and R. M. Drake, Jr. Heat and Mass Transfer, 2nd ed. McGraw-Hill, New York, N. Y. (1959)

(11) Forster, H. K. and N. Zuber. Amer. Inst. Chem. Engrs. Journal, 1, No. 4, (1955) 531-35.

(12) Gambill, W. R., R. D. Bundy, and R. W. Wansbrough. "Heat Transfer, Burnout, and Pressure Drop for Water in Swirl Flow Through Tubes with Internal Twisted Tapes." Chem. Engr. Progr. Symp. Series, 57, No. 32, (1961) 127-37.

(13) Gambill, W. R. and N. D. Greene. "Boiling Burnout with Water in Vortex Flow." Chem. Engr. Progr., 10, (1958) 68-76.

(14) Gouse, S. W. and C. D. Andrysiak. "Some Observations on Two-Phase Flow Oscillations." Multi-Phase Flow Symposium, Amer. Soc. Mech. Engrs., New York, (1963) 84-89.

(15) Hawthorne, W. R. "Secondary Circulation in Fluid Flow." Proc. Roy. Soc. London, A, 206, (1951) 374.

(16) Hendricks, R. C. and F. F. Simon. "Heat Transfer to Hydrogen Flowing in a Curved Tube." Multi-Phase Flow Symposium, Amer. Soc. Mech. Engrs., New York, (1963) 90-93.

(17) Ito, H. "Friction Factors for Turbulent Flow in Curved Pipes." J. Basic Engr., Trans. Amer. Soc. Mech. Engrs, D, 81, (1959) 123-34.

(18) Jenkins, R. (unpublished M. Ch. E. thesis, Univ. of Delaware, 1947)

(19) Jeschke, D. "Heat Transfer and Pressure Loss in Coiled Pipes." Ergaenzungsheft Z. Ver. dtsch. Ing., 69, (1925) 24-28.

(20) Keenan, J. H. and F. G. Keyes. Thermodynamic Properties of Steam, 1st ed., 26th printing. John Wiley, New York, N. Y. (1954)

(21) Kirpikov, A. V. "Heat Transfer in Helically Coiled Pipes." Trudi Moskov. Inst. Khim. Mashinojtrojenija, 12, (1957) 43-56.

(22) Koutsky, J. A. and R. J. Adler. "Minimization of Axial Dispersion by Use of Secondary Flow in Helical Tubes." Canadian J. of Chem. Engr., 42, (1964) 239-46.

(23) Kreith, F. "The Influence of Curvature on Heat Transfer to Incompressible Fluids." Trans. ASME, 77,

(1955) 1247-56.

(24) Kubair, V. and N. R. Kuloor. "Heat Transfer to Newtonian Fluids in Coiled Pipes in Laminar Flow." Int. J. Heat Mass Transfer, 9, (1966) 63-75.

(25) Lockhart, R. W. and R. C. Martinelli. "Proposed Correlation of Data for Isothermal Two-Phase, Two-Component Flow in Pipes." Chem. Engr. Prog., 45, (1949) 39-48.

(26) Perry, J. H., ed. Chemical Engineers' Handbook, 3rd ed. McGraw-Hill, New York, N. Y., (1950) 374.

(27) Rippel, G. R., C. M. Eidt, Jr., and H. B. Jordan, Jr. "Two-Phase Flow in a Coiled Tube." Ind. Engr. Chem., Process Design and Development, 5, No. 1, (1966) 32-39.

(28) Rogers, G. F. C. and Y. R. Mayhew. "Heat Transfer and Pressure Loss in Helically Coiled Tubes with Turbulent Flow." Int. J. Heat Mass Transfer, 7, (1964) 1207-16.

(29) Rohsenow, W. M. "Heat Transfer—A Symposium." Engineering Res. Inst., Univ. of Michigan, Ann Arbor, Mich. (1952)

(30) Rohsenow, W. M. Trans. Am. Soc. Mech. Engrs., 74, (1952) 969.

(31) Schrock, V. E. and L. M. Grossman. "Forced Convection Boiling in Tubes." Nuclear Science and Engr., 12, (1962) 474-481.

(32) Seban, R. A. and E. F. McLaughlin. "Heat Transfer in Tube Coils with Laminar and Turbulent Flow." Int. J. Heat Mass Transfer, 6, (1963) 387-95.

(33) Wattendorf, F. L. "A Study of the Effect of Curvature on Fully Developed Turbulent Flow." Proc. Roy. Soc. London, A, 148, (1934) 565-98.

(34) White, C. M. "Streamline Flow Through Curved Pipes." Proc. Roy. Soc. A, 123, (1929) 645-63.

(35) Woods, W. K. (unpublished Sc. D. thesis, Mass. Inst. Technol., Cambridge, Mass. 1940).
see also:
McAdams, W. H. Heat Transmission, 3rd ed. McGraw-Hill, New York, N. Y., (1954) 398.

(36) Yudovich, Amos. "Forced Convection Boiling in a Coil." (unpublished M. S. thesis, Oklahoma State University, 1966).

APPENDIX A

VARIATION OF WALL THICKNESS AND HEAT GENERATION AROUND THE CIRCUMFERENCE OF A COILED TUBE

In the process of forming a straight tube into a coil, the concave side of the coil is stretched while the tube wall on the convex side is made thicker. Furthermore, the tube cross-section assumes an elliptical shape. The extent of this ellipticity depends on the method of filling and bending the tube as well as the rheology of the tube material. The ratio of the major to the minor diameter was 0.637/0.619 for the small coil and 0.631/0.625 for the large coil.

If the ellipticity of the tube is neglected and if the bending strain does not cause a change in the density of the tube material, the following relations can be written

$$\delta_m R\alpha = \delta (R - r_m \sin\phi)\alpha \qquad \text{(A-1)}$$

where α is the angle enclosing the arc under consideration (Fig. A-1), δ is wall thickness at the angular position ϕ, and δ_m is wall thickness at $\phi = 0$, i.e., the wall thickness of the straight tube. Thus

$$\delta = \delta_m \left(\frac{R}{R - r_m \sin\phi} \right) \qquad \text{(A-2)}$$

Now consider two elements of volume each of which has a cross-sectional area of ϵ and each of which extends throughout the arc α. The length of the element located at the

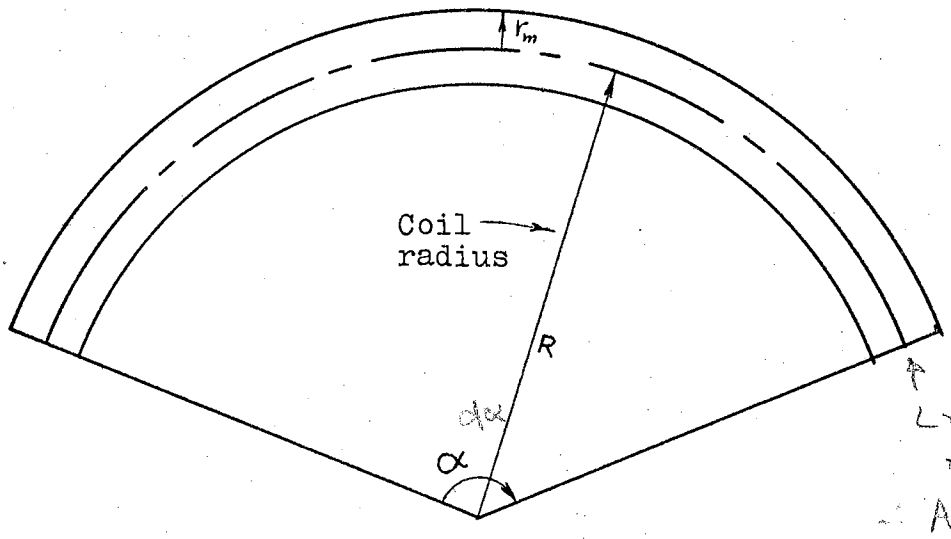

Fig. A-1a A Segment of Coil

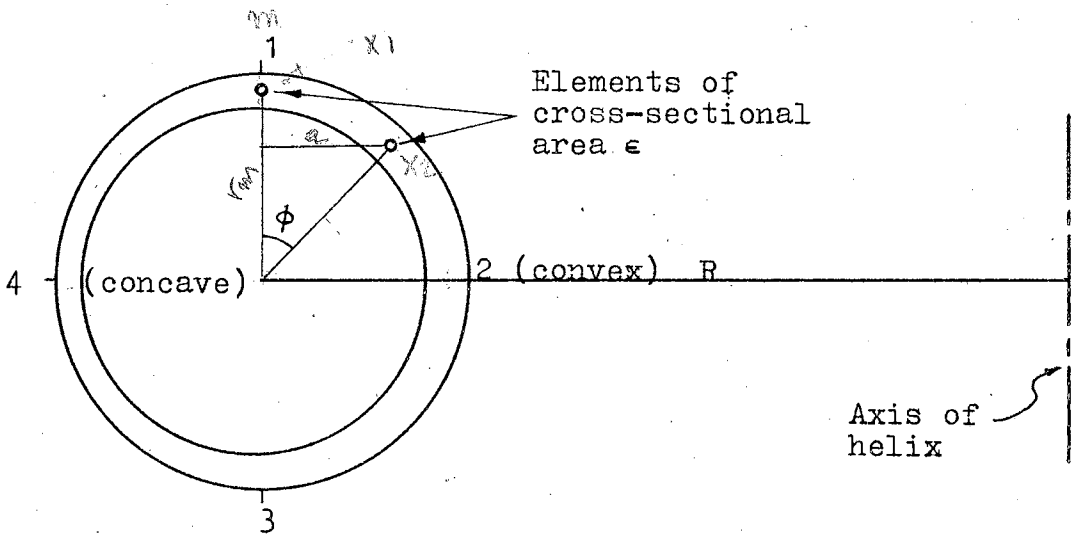

Fig. A-1b Tube Cross-Section

Fig. A-1 Variation of Wall Thickness Around Circumference of a Coiled Tube

angular position ϕ is given by

$$L = L_m\left(\frac{R - r_m \sin\phi}{R}\right) \qquad (A\text{-}3)$$

where L_m is the length of the element located at the angular position $\phi = 0$. Since these two elements have the same cross-sectional area, their electrical resistance is proportional to their length. Therefore,

$$\mathcal{R} = \mathcal{R}_m\left(\frac{R - r_m \sin\phi}{R}\right) \qquad (A\text{-}4)$$

The electric potential across these two elements is the same; so the current intensity and the power dissipated in these two elements are related by

$$I = I_m\left(\frac{R}{R - r_m \sin\phi}\right) \qquad (A\text{-}5)$$

and

$$\mathcal{R} I^2 = \mathcal{R}_m I_m^2\left(\frac{R}{R - r_m \sin\phi}\right) \qquad (A\text{-}6)$$

Dividing both sides of equation (A-6) by ϵL, we get

$$G = \frac{\mathcal{R}_m I_m^2}{\epsilon L}\left(\frac{R}{R - r_m \sin\phi}\right)$$

$$= \frac{\mathcal{R}_m I_m^2}{\epsilon L_m}\left(\frac{R}{R - r_m \sin\phi}\right)^2$$

$$= G_m\left(\frac{R}{R - r_m \sin\phi}\right)^2 \qquad (A\text{-}7)$$

The maximum deviation of δ from δ_m is 5.7 per cent for the small coil and 2.8 per cent for the large coil. The maximum deviation of G from G_m is 11.8 per cent for the small coil and 5.7 per cent for the large coil.

Finally, G_m is assumed to be equal to the power input to the coil, per unit volume, as measured experimentally.

The fact that the tube wall is distorted must be

considered when calculating the circumferential average heat transfer coefficient; the inner wall is shrunk while the outer wall is stretched. In order to include this correction, albeit small, the convex side heat transfer coefficient must be multiplied by

$$\frac{\int_{\pi/4}^{\pi/2} \left(\frac{R - r_m \sin\phi}{R}\right) r_m \, d\phi}{\int_{\pi/4}^{\pi/2} r_m \, d\phi} = 0.949 \text{ for the small coil}$$

$$= 0.975 \text{ for the large coil,}$$

while the concave side heat transfer coefficient must be multiplied by

$$\frac{\int_{0}^{\pi/4} \left(\frac{R + r_m \sin\phi}{R}\right) r_m \, d\phi}{\int_{0}^{\pi/4} r_m \, d\phi} = 1.051 \text{ for the small coil}$$

$$= 1.025 \text{ for the large coil.}$$

Therefore, the circumferential average heat transfer coefficient for the small coil is calculated by

$$\bar{h} = (h_1 + 0.949\, h_2 + h_3 + 1.051\, h_4)/4 \qquad \text{(A-8)}$$

and for the large coil by

$$\bar{h} = (h_1 + 0.975\, h_2 + h_3 + 1.025\, h_4)/4. \qquad \text{(A-9)}$$

In the above two equations the subscripts on h refer to the positions around the circumference.

VITA

Ali Owhadi

Candidate for the Degree of

Doctor of Philosophy

Thesis: BOILING IN SELF-INDUCED RADIAL ACCELERATION FIELDS

Major Field: Chemical Engineering

Biographical:

Personal Data: Born in Rafsendjan, Iran, November 11, 1931, the son of Mehdi and Fatima Owhadi.

Education: Attended grade school in Rafsendjan, Kerman, and Teheran, Iran; graduated from Alborz High School (Teheran) in 1949; received the Bachelor of Science and the Master of Science degrees from the University of Michigan in February, 1955, and June, 1956, respectively, with a major in Chemical Engineering; completed requirements for the Doctor of Philosophy degree in July, 1966.

Professional experience: Employed as Process Design Engineer with John G. Hoad and Associates, Consulting Engineers in Ypsilanti, Michigan, 1956-1957; served two years as Process Development Engineer in Velsicol Chemical Corporation in Chicago, Illinois, 1957-1959; employed for eighteen months as Plant Engineer with Pars Oil Company in Teheran, Iran, 1961-1963.